Faculty of Mechanical Engineering

TRIBOLOGICAL PERFORMANCES FOR PALM KERNEL ACTIVATED CARBON EPOXY COMPOSITE

Noor Ayuma Binti Mat Tahir

Master of Science in Mechanical Engineering

2016

TRIBOLOGICAL PERFORMANCES FOR PALM KERNEL ACTIVATED CARBON EPOXY COMPOSITE

NOOR AYUMA BINTI MAT TAHIR

A thesis submitted
In fulfilment of the requirements for the degree of
Master of Science in Mechanical Engineering

Faculty of Mechanical Engineering

UNIVERSITI TEKNIKAL MALAYSIA MELAKA

2016

DECLARATION

I declare that this thesis entitled “Tribological Performances for Palm Kernel Activated Carbon Epoxy Composite” is the result of my own research except as cited in the references. The thesis has not been accepted for any degree and is not currently submitted in candidature of any other degree.

Signature	:	………..
Name	:	………………………………….......
Date	:	………………………………….......

APPROVAL

I hereby declare that I have read this thesis and in my opinion this thesis is sufficient in terms of scope and quality for the award of Master of Science in Mechanical Engineering.

Signature : ……………………………………………..

Supervisor's Name : …………………………………………….

Date : ……………………………………………

DEDICATION

To my beloved mother and father

ABSTRACT

Nowadays, it is expected that for most materials to be environmental friendly. Waste materials may be considered a secondary source of materials with an energetic advantage due to its high energy content. Consisting of a carbon material from agriculture wastes as new reinforcement substitutes in the fabrication of polymer matrix composites, are supposed to have large potential for a zero waste strategy in improving tribological properties at an affordable cost. Until today, based on our knowledge and from the literature review, there is no study regarding the potential of Palm Kernel Activated Carbon (PKAC) as solid lubricant in polymer matrix composites. Thus, a study on carbon materials from agriculture wastes has a great potential in tribological applications. The objectives of this study were to investigate the tribological performance of Palm Kernel Activated Carbon Epoxy composites and its wear mechanisms, and proposed wear and friction equations using Analysis of Variance (ANOVA). Basically, the composite were formed into pin shaped sizing of 30 mm height and 10 mm diameter using compaction technique. When the pin were ready, basic mechanical test were done. Then the pin were tested through pin-on-disc tribometer, then the surface morphology of the pin were studied through Scanning Electron Microscope (SEM) and Energy Dispersive Xray (EDX). The collected data were analysed through qualitative and quantitative approaches. From the study, it is interesting to find that the coefficient of friction and wear rate of the composite are highly affected by the composition and temperature due to the failure of the Epoxy bond. In addition, some traces of transfer layer were also found. Through comparison between friction and wear equations proposed with the experimental value, the equations shows average of 90.70% of reliability. Thus it can be said that the PKAC-E composite has high potential as the self-lubricating materials.

ABSTRAK

Bahan yang diguna pakai pada masa kini adalah sudah dijangkakan sebagai bahan mesra alam. Bahan buangan boleh diguna pakai sebagai bahan sumber kedua kerana bahan tersebut mempunyai kelebihan untuk beroperasi dengan kadar tenaga tambahan yang diperolehi dari kandungan tenaga yang tinggi. Bahan buangan agrikultur yang mengandungi karbon sebagai bahan penguat tambahan didalam komposit polimer adalah dijangkakan untuk mempunyai potensi yang besar sebagai bahan bebas pencemaran. Potensi bahan tersebut mempunyai kebaikan dalam menambah baik ciri-ciri tribologi dalam kadar yang berpatutan. Bedasarkan pengetahuan umum dan kajian sebelum ini, masih tiada lagi kajian berkaitan karbon aktif dari biji kelapa sawit sebagai pelincir keras didalam komposit polimer. Oleh yang demikian, kajian terhadap bahan karbon dari hasil buangan agrikultur mempunyai potensi besar terhadap aplikasi dalam bidang tribologi. Tujuan kajian ini adalah untuk mengkaji prestasi tribologi terhadap karbon aktif dari biji sawit bersama epoksi serta mekanisma haus komposit tersebut dan mengetengahkan model kehausan dan geseran menggunakan aplikasi ANOVA. Secara dasarnya, komposit dibentuk menjadi pin bersaiz 30mm tinggi serta 10mm diameter melalui teknik tekanan. Apabila pin tersebut telah siap, ujian mekanikal mudah dijalankan. Kemudian, pin diuji menggunakan ujian "pin-on-disc" lalu permukaan yang bercalar dan haus di analisis menggunakan "Scanning Electron Microscope" SEM dan "Electron Dispersive Xray" EDX. Data yang diperolehi dianalisis menggunakan pendekatan kualitatif dan kuantitatif. Berdasarkan hasil dapatan dari kajian, kadar tetapan geseran and kadar kehausan dari komposit tersebut adalah sangat dipengaruhi oleh kadar suhu dan komposisi berikutan kegagalan yang berpunca dari pegangan elemen epoksi. Selain dari itu, sebahagian kesan lapisan bahan yang terpindah juga berjaya dikesan. Melalui perbandingan antara persamaan kadar geseran dan kadar kehausan terhadap nilai kajian, model tersebut memaparkan purata sebanyak 90.70% kadar kebolehpercayaan. Oleh yang demikian, adalah wajar untuk mengatakan bahawa komposit PKAC-E berpotensi sebagai bahan pelincir sendiri.

ACKNOWLEDGEMENTS

First and foremost, I would like to take this opportunity to express my sincere gratitude to my supervisor Assoc. Prof. Dr. Mohd Fadzli Bin Abdollah for his nonstop supervision, support, motivation, encouragement, and immense knowledge towards the completion of research and thesis writing.

I would also like to express my gratitude to Dr. Rafidah Binti Hassan as co-supervisor of this project for her unlimited advice and suggestions. Also to my deepest thanks to the Ministry of Education Malaysia for supporting this research by the grant (Grant No.: ERGS/2013/FKM/TK01/UTEM /02/04/E00016) and scholarship from MyBrain15.

Special thanks to the members of the Green Tribology and Engine Performance (G-TriboE) research group from CARe UTeM, and my colleagues especially Dr. Muhammad Ilman Hakimi Chua Bin Abdullah for his advices and guides. I would also like to express my deepest gratitude to Dr. Nor Azmmi Bin Masripan, for his contribution on giving ideas in every colloquium, Dr. Mohd Zulkefli Bin Selamat for giving ideas and solution on designing mould, all the technicians from the laboratory Faculty of Mechanical Engineering for their assistance and efforts in all the lab and analysis works.

Special thanks to my family and friends for their moral support in completing this project. Lastly, thank you to everyone who are not listed here who had been to the crucial parts of realization of this project.

TABLE OF CONTENTS

LIST OF TABLES

LIST OF FIGURES

LIST OF ABBREVATIONS AND SYMBOLS

θ	-	Angle (degree)
m	-	Mass
g	-	Gravity
nm	-	Nanometer
Σ	-	Summation
wt%	-	Weight Percent
µm	-	Micrometer
σ	-	Stress
ε	-	Strain
ρ	-	Density
T	-	Temperature
C	-	Composition
Ra	-	Surface Roughness
F	-	Applied Load
k	-	Specific Wear Rate
S/N	-	Signal to Noise Ratio
Cont %	-	Contribution Percent
COF	-	Coefficient of Friction
RPM	-	Rotation per Minutes
PKAC	-	Palm Kernel Activated Carbon
PKAC-E	-	Palm Kernel Activated Carbon reinforced Epoxy
SEM	-	Scanning Electron Microscope
EDX	-	Energy Dispersive Xray
DLC	-	Diamond Like Carbon
MMC	-	Metal Matrix Composite
PMC	-	Polymer Matrix Composite

LIST OF PUBLICATIONS

<u>**Article in Journals:**</u>

Mat Tahir, N.A., Abdollah, M.F.B., Hassan, R., Amiruddin, H. and Abdullah, M.I.H.C., 2016. Statistical Models for Predicting Wear and Friction Coefficient of Palm Kernel Activated Carbon-Epoxy Composite using the ANOVA. *Industrial Lubrication and Tribology*. ISI Q4 (Accepted for publication)

Mat Tahir, N.A., Abdollah, M.F.B., Hassan, R. and Amiruddin H., 2016. The effect of sliding distance at different temperatures on the tribological properties of a palm kernel activated carbon-epoxy composite. *Tribology International*, 94, pp. 352-359.
ISI Q1 (DOI: http://dx.doi.org/10.1016/j.triboint.2015.10.001).

Mat Tahir, **N.A.,** Abdollah, M.F.B., Hasan, R. and Amiruddin, H., 2015. The effect of temperature on the tribological properties of palm kernel activated carbon-epoxy composite. *Tribology Online*, 10. 6, pp. 428-433. SCOPUS (DOI: http://doi.org/10.2474/trol.10.428).

Chua, K.W., Abdollah, M.F.B., **Mat Tahir N.A.,** and Amiruddin, H., 2015. Frictional properties of palm kernel activated carbon-epoxy composite under various normal loads. *Jurnal Teknologi (Sciences and Engineering),* 76, pp. 1-4. SCOPUS
(DOI: http://dx.doi.org/10.11113/jt.v76.5783).

Conferences Attended:

Mat Tahir, N.A., Abdollah, M.F.B., Hassan, R. and Amiruddin, H., 2014. The effect on friction coefficient and wear rate of palm kernel activated carbon-epoxy (PKAC-E) composite at different temperatures. *Proceedings of 3rd Malaysia-Japan Tribology Symposium*, Kuala Lumpur, 12~14 November 2014.

Mat Tahir, N.A., Abdollah, M.F.B., Hassan, R. and Amiruddin, H., 2014. The effect of sliding distance on friction coefficient and Wear rate of palm kernel activated carbon-epoxy (PKAC-E) composites. *Proceedings of 2nd Advance Materials Conference*, Langkawi, 25~26 November 2014.

Competition Attended:

Mat Tahir, N.A., Abdollah, M.F.B., Hassan, R., Amiruddin, H., and Abdullah, M.I.H.C., 2016. Tribological performances for palm kernel activated carbon epoxy (PKAC-E) composites. *Tribology Poster Competition*, Universiti Malaya, Kuala Lumpur, 01 June 2016.

Awards:

Gold and Special Jury Award; Agro-waste for sustainable self-lubricating materials. UTeMEX2015 (Green Technology Category). *UTeM Research and Innovation Expo 2015*, Universiti Teknikal Malaysia Melaka, Melaka, 27~28 October 2015.

CHAPTER 1

INTRODUCTION

1.1 Background

Palm kernel activated carbon is actually the waste from palm oil extraction process. As shown in Figure 1.1, the palm oil is actually made up of exocarp, mesocarp, endocarp, and endosperm. After the extraction process, what is actually left to become activated carbon is the endocarp part, which is called the kernel. Through the extraction process, the potential of this kernel or endocarp is found through the ash content, the moisture content, and the physical condition—that is, high density, hardness, and volatile content.

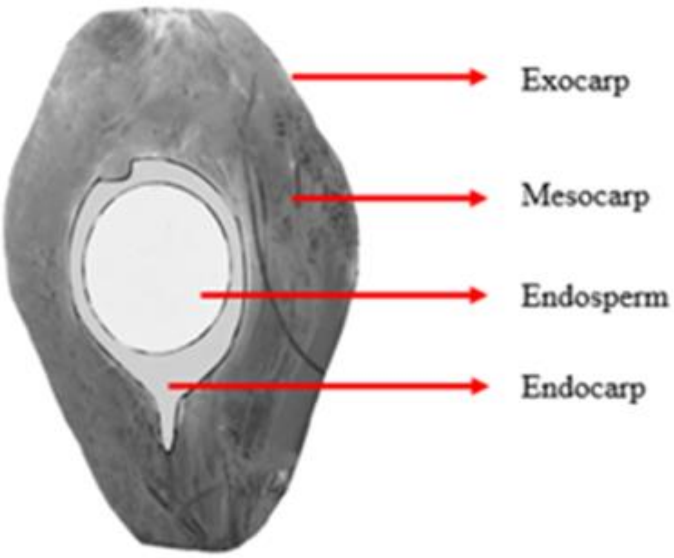

Figure 1.1 Components of palm oil fruit
[Source: http://www.bgrimmgreenpower.com/biodisel-sourcing.php]

Ash content can lead to increase hydrophilic ability and can have catalytic effects as well, causing restructuring process during regeneration of used activated carbon. The inorganic material contained in activated carbon is measured as ash content, generally in the range of 2 to 10%. Moreover, some activated carbons can absorb considerable moisture from over 25 to 30% for over a month under humid conditions, but maintain to appear dry. Although this obviously dilutes the carbon, sometimes, the moisture content does not affect the absorptive power of active carbons at all.

Recently, a significant shift to oil palm is an acknowledged emerging trend in the cooking oil industry. From Figure 1.2, it can be seen that Malaysia and Indonesia are leading other countries in the world's palm oil production. As global players in the palm oil market, it can be expected that there will be a huge abundance of palm oil waste or biomass in both countries. However, this waste may be reused in consideration that biomass can be recycled and transformed into potentially marketable value-added products with the help of additives and other materials.

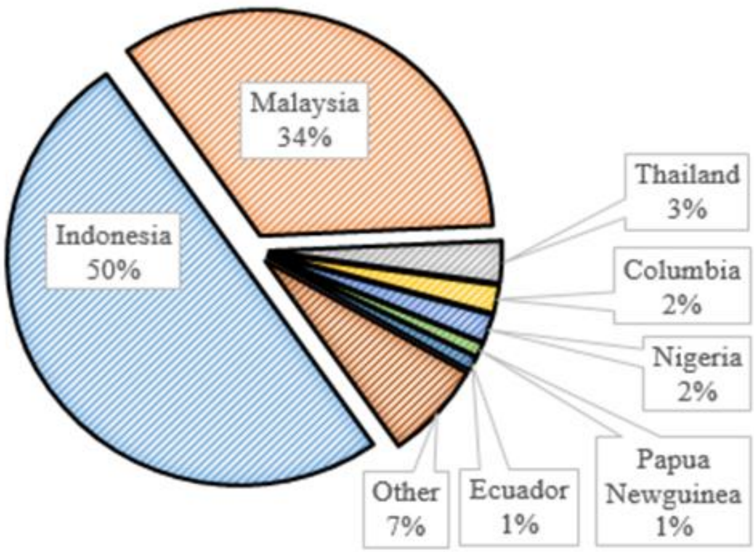

Figure 1.2 Distribution of palm oil worldwide in 2013
[Source: GreenPalm at slideshare.net]

1.2 Problem Statement

It has become a whole wide problem that friction and wear causing a huge amount of loss. The need to reduce friction and wear in the automotive industry to obtain maximum efficiency—while at the same time being environment-friendly by reducing waste—consistently creates an increasing demand for research in Tribology, especially in lubrication. Accordingly, presenting more efficient lubrication or self-lubricating materials may be the solution in overcoming these problems.

Nowadays, studies on carbon reinforced with various types of matrix as reinforcement has become popular as an alternative to current lubricating materials has become an attraction in Tribology field. Studies on the use of natural products such as fibre into composites have already been done by a number of researchers such as Nirmal et. al (2015) and Bakry et. al (2013). However, there is a research gap on the use of waste as self-lubricating materials.

It is noted that carbon may come in many forms such as fibres, flakes, tubes, and more [Brostow et. al (2010), Luo (2013), and Zamri and Shamsul (2011)]. In addition, amorphous carbon were found as waste product of palm oil seed, which is called activated carbon [Zamri et. al (2011)]. According to Zamri et. al (2011), activated carbon has the potential to act as a self-lubricating agent when reinforced with aluminium. It would be highly beneficial if these unique properties of carbon can be used as self-lubricating agents for reducing friction and wear besides reducing the waste product from the oil extraction process.

Meanwhile, oil extraction process from palm oil produces lots of waste that may become a problem on later days. This waste has potentials to become self-lubricating materials due to its residual oils, but with transformation as activated carbon.

To summarize, the need to maintain optimal function of automotive machines is a pressing issue that calls for efficient solutions. The direction is to recycle waste product, particularly of palm oil into self-lubricating materials. It is also a sustainable and environment-friendly alternative.

1.3 Objectives

The study objectives were largely influenced by findings from other previous studies as well as anchored on the potential of carbon in reducing friction and wear. The scope and limitations of the study further de-limits the study to the following objectives:

a) To investigate the tribological behaviour of palm kernel activated carbon reinforced epoxy composite at different temperatures and sliding distance;

b) To identify the predominant wear mechanisms of palm kernel activated carbon reinforced epoxy composite under dry sliding conditions;

c) To propose mathematical equations for friction and wear of palm kernel activated carbon reinforced epoxy composite using ANOVA.

1.4 Scope

This research is limited to the study of palm kernel activated carbon (PKAC) reinforced epoxy (E). Specifically, the parameters studied were sliding temperature ranging from 27 °C (room temperature) up to 150 °C. Meanwhile the sliding distance ranging from 500 m to 2500 m, sliding speed ranging from 500 m to 1750 m, composition of PKAC ranging from 60 % to 75 %, surface roughness (Ra) ranging from 0.2 µm to 0.8 µm, and applied load ranging from 19.62 N to 49.05 N. The details on selected ranges were discussed in chapter 3.3.

Accordingly, the work done in this study was divided into several stages. First, the samples were prepared using the compaction method, after which the specimens were subjected to hardness and density tests. After arriving at a suitable composition, the composites were first tested on the pin-on-disc tribometer testing or tribological test at different temperatures and sliding distances. It should be noted that these tests were done in order to analyse the behaviour of the composites under high temperature, and additionally, evaluate the effect on the composites at different sliding distances, including its effect on the sliding disc.

Likewise, the surface morphology of the worn surface was taken under Scanning Electron Microscopy (SEM) and energy dispersive X-ray (EDX) to determine chemical composition contents. Finally, data results from the tests were utilised to propose both wear and friction equation using Analysis of Variance or ANOVA. In addition, the Minitab statistical software was used to design the orthogonal arrays.

1.5 Thesis Structure

This thesis specially describes the effect on coefficient of friction and wear rate of PKAC-E on dry sliding conditions following ASTM G99 standards. There are five chapters briefly outlined as shown in Figure 1.3. The chapters of this paper are as follows:

Chapter 1 is an introduction to the potential of palm kernel activated carbon—a by-product of the growing palm oil industry— as a self-lubricating. In addition, this chapter describes the problems, purpose and objectives as well as the scope of the study.

Chapter 2 aims to clarify the importance as well as the need to understand tribological issues with a brief history of Tribology and basic theories on lubrications. In addition, this section discusses the effects of coefficient of friction and wear on metal matrix composite and polymer composite, including additional information on PTFE and DLC.

Chapter 3 gives a detailed description of the procedure and flow of the study. Related figures, tables, and illustrations in this chapter are in the Appendix.

Chapter 4 presents the findings of the study. Data results from the tests were interpreted from the context of some lubrication theories as well as by building on the findings of other related studies. The qualitative approach was used in the interpretation of data based on the observations from the surface morphology image while quantitative analysis, specifically, analysis of variance or ANOVA was used to interpret friction and wear data that was used to build the wear and friction model.

Lastly, Chapter 5 presents a summary of the major findings of this work and its implications for current research. In addition, through knowledge generated by the study, the authors suggest further research that can expand the field of study on using waste products as alternative sources for active carbon-based lubricating materials.

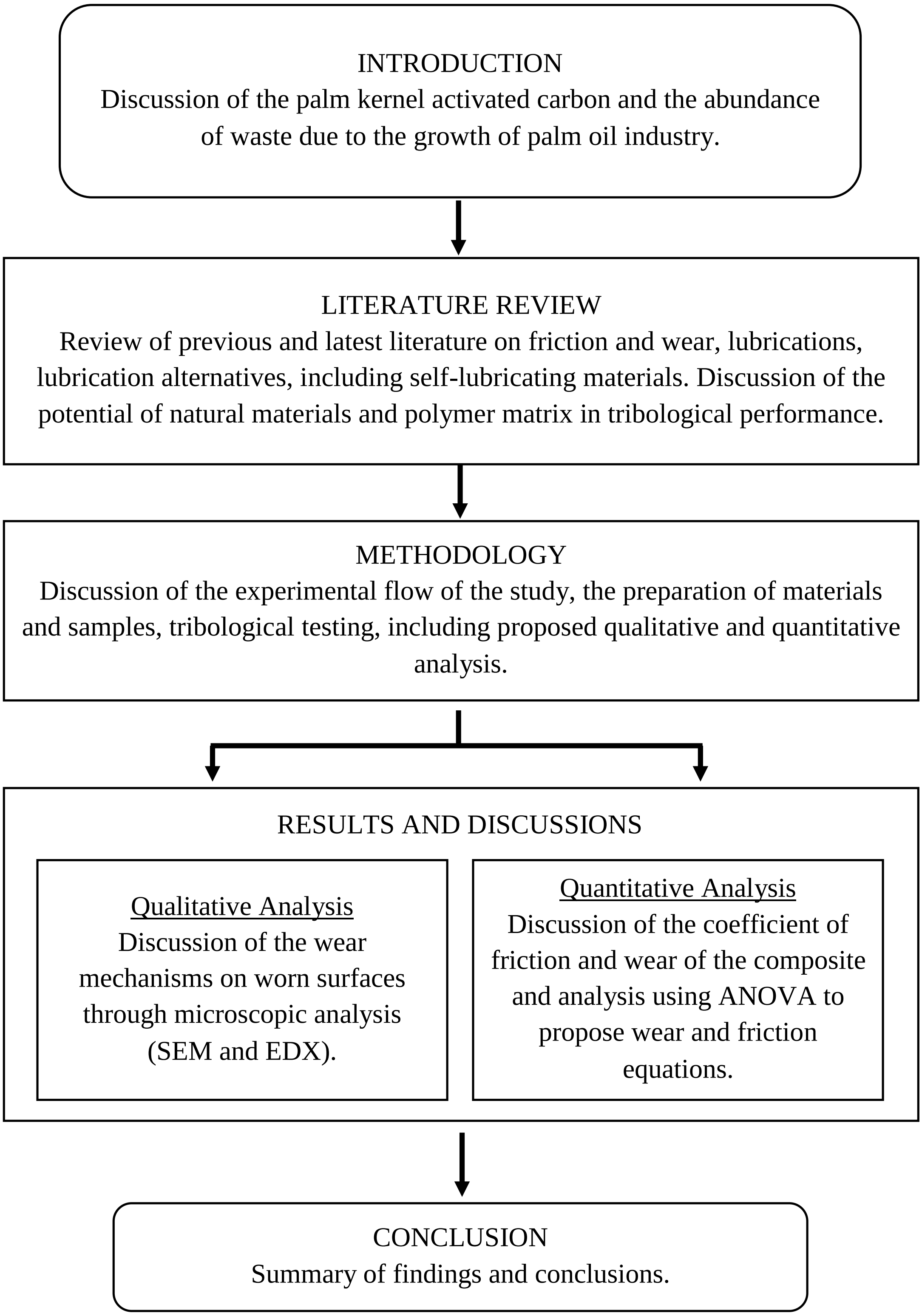

Figure 1.3 Thesis flow structure

CHAPTER 2

LITERATURE REVIEW

2.1 Demand for a Better Automotive Technology

In 2014, the Government of Malaysia released a policy statement regarding its new perspective for the automotive industry. Under the National Automotive Policy, the government announced that Malaysia will now implement as well as promote energy efficient vehicles or EEVs particularly, in the production of national car. Moreover, the government set the target at year 2020 for the EEVs to meet standard terms of carbon emission level and fuel consumption (Dasar Automotif Nasional, 2014).

Consequently, and as a response to the government's policy thrust for the automotive industry, demand for a more efficient automotive industry was urgently raised. One of the solutions is to create a more efficient engine.

As a fact, according to Holmberg et. al (2012), only 21.5 % of the energy combusted in the engine were actually used to move a car. He also explained that the loss of energy were categorised into loss to the exhaust, loss due to cooling process, and also mechanical power. The mechanical power were then divided into friction loss and air drag resistance. From the friction loss percentage, 11.5% were loss at the engine, 5 % at the transmission, 11.5 % at the rolling resistance and remaining 5% at the brakes. The friction at the rolling resistance, the brakes, and also the air drag were impossible to be eliminated as it is important to move the car. In this case, there a plenty of room of energy loss in a single car. The breakdown of the energy consumption were shown in Figure 2.1. Hence, it is wise to say that even if a small improvement is made, the efficiency of the engine would be increased.

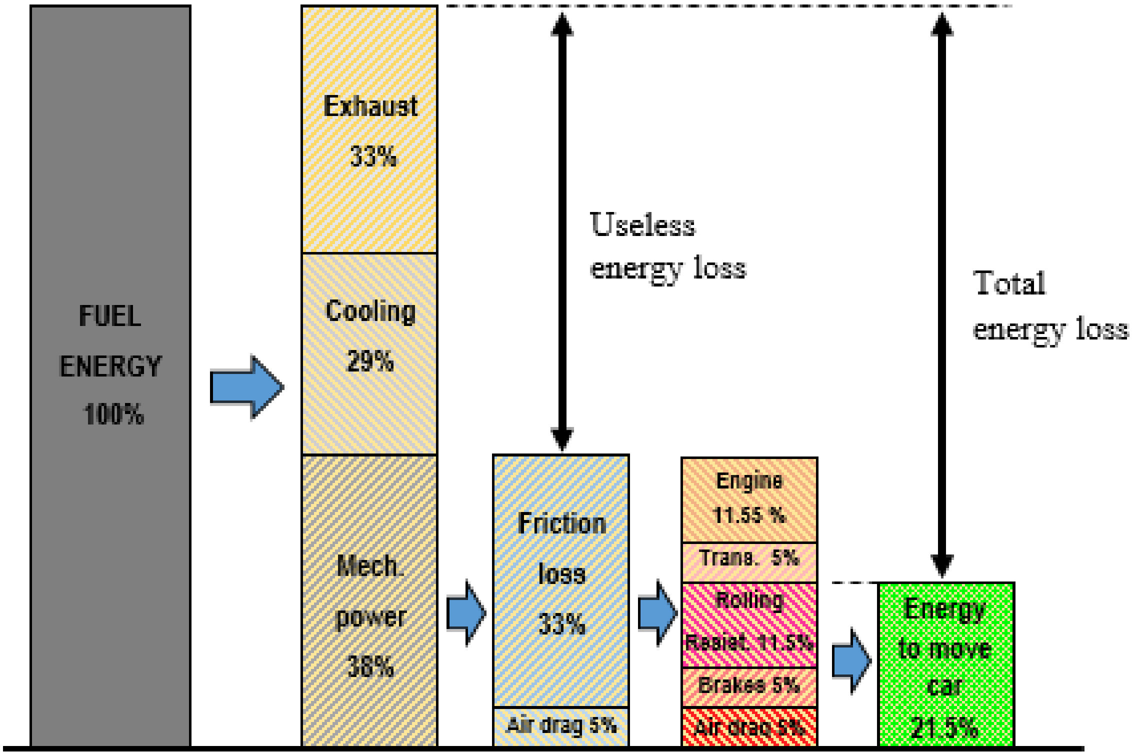

Figure 2.1 Breakdown of a passenger car energy consumption
[Source: Holmberg et. al (2012)]

From Figure 2.1, it can be seen that the total of energy loss were three times bigger than the energy used to move a car. One of the methods to increase the efficiency of an engine is by reducing the energy loss due to mechanical interactions in the system. The mechanical interactions in the engine, which is the focus of this study, are essentially the friction and wear between moving parts of the engine, including components such as bearings, clutches, and pistons.

There is no doubt that the reduction in fuel consumption is indeed an important task as well as a challenge to all engineers. Besides reducing the cost of maintaining a car, the fuel reserves become manageable as well when the percentage of fuel demand is slightly lower for every car. Hence, this issue has direct impact on the need to find a more efficient lubrication system for components and engines that is, at the same time, environment-friendly.

According to Zhao et al. (2014), improvements in current lubrication are also important from the environmental point of view, considering that current lubrication products are not biodegradable, and additionally, most cars require high maintenance and wear off after certain cycles.

2.2 Lubrication Theory and Bearing Technology

The main purpose of lubrication is to reduce wear. In addition, a lubricant is also used as a heat reduction system between the contacting surfaces. Lubricants act as a protective film, allowing the two surfaces in contact to stay separated. The separation lessens the friction and heat between the motions of the two surfaces. As a result, the wear and tear of parts are reduced. This, in turn, results in lesser number of parts to be repaired or replaced, along with longer life cycles of the parts and components. Lubrication is also used to reduce oxidation, and hence prevent rust. According to Nosonovsky and Bushan (2012) sometimes, lubrication is used as insulation in components.

The promising future of the lubrication era was initiated in 1842 by Osborne Reynolds. His research focused on rotating shaft and bearings. Reynolds observed that the rotating shaft pulled a converging force between the shaft and the bearing. Due to the viscous properties of lubrication, the lubricants provided sufficient liquid pressure between the bearing and the shaft wedge to create separation between the two surfaces. Supporting Reynolds' findings, the Stribeck curve summarises the lubrication regimes by connecting the relation between the affecting parameters.

Previous research focused on various lubrication systems, including gas lubrication, solid lubrication, and also liquid lubrication. Dowson (1998) states that earlier civilisations used animal fats as a method to reduce friction. This shows that the era of lubrication started way back before the invention of machines, and basic lubrication principle was applied to reduce friction in daily life. Bowman and Stachowiak (1996) reported that there was a steady development in the application of lubricants in daily life from the mid-1400s, but it was only starting in the 1750s that the value and potential of lubricants were recognised for the reduction of friction and wear.

Much research has been done lately on the quest for a better lubrication system. This includes the lubrication on the mechanical contacts between parts and also in the engine oil itself. Haq and Bibi (2007) studied the possibility of creating lubrication alternatives from vegetable oils. They found out that higher viscosity and lower iodine value may affect the tribological performance of the engine oil. Vegetable oils are known to possess a unique ability of being a good anti-wear material.

Abdullah et al. (2013) found that lower coefficient of frictions (COF) in engines can be achieved through the addition of nanoparticles and surfactant in the standard engine oil. The friction in engines can be reduced by altering the current composition and viscosity of the operating oil. Thus, constant improvements can reduce the COF in engines, possibly leading to lower fuel consumption.

Besides improving the engine oils, the researchers also presented a few more improvement methods. For instance, another alternative offered by Abdollah et al. (2013) was replacing grease and oil in bearings with nitrogen and oxygen gas. It was noted that almost 24% of COF could be reduced by applying nitrogen gas into the bearings. This was because the nitrogen gas inside the bearings was able to maintain the distance between the bearings, holding them from having maximum contact with each other by creating a constant pressure of the gas.

From a general perspective, it can be seen that there was a positive progress in creating a lower COF system. However, there still are some gaps and room for improvement due to certain weaknesses in the current process of lubrication development. For example, according to Nosonovsky and Bushan (2012), gas lubrications may leak and they also have lower pressure resistance compared to liquid and solid lubrications. This is due to the gap between the atoms, which are wider compared to solid. Alongside the oil engine alternatives, there might be few stepping-stone improvements.

Lubrication can be grouped into liquid, solid, and gas types. Lubrication is introduced between two contacting surfaces to act as a boundary film between those surfaces. In other words, the asperities between the surfaces are not touching each other technically. Figure 2.2 illustrates the presence of lubrication between two contacting surfaces.

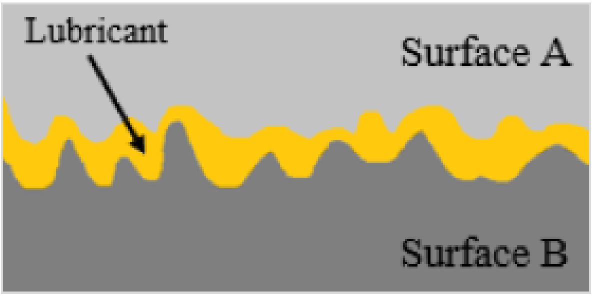

Figure 2.2 Lubrication between two contacting surface
[Source: Ludema (1996)]

Ahmed and Nassar (2013) proposed a solution to eliminate heat due to friction by introducing a cooling reservoir in the system. By cycling the lubricant through the reservoir, the viscosity of the fluid can be maintained. Another method suggested by the authors involved introducing additive in the lubrication mixture. Addition of an additive may reduce the dependence of viscosity towards temperature. This is because, at low temperatures, the molecule chain contracts and does not impact the fluid viscosity. At high temperatures, the chain relaxes and the viscosity change. This is because the fluid film formation is influenced by:

a) The contact surfaces need to meet at a certain range of angle between the surfaces to allow formation of the lubricant wedge.
b) The contact surfaces must be smooth. Sharp surfaces would disrupt the fluid film. The fluid viscosity must be high to maintain adequate film thickness.
c) The fluid must adhere to the contact surfaces for facilitating conveyance into the pressure area to support the load.

d) The fluid must distribute itself completely within the contact area.

Organic compounds with complex long-chain molecules are deemed the best additives. These long chains are able to bind tightly with each other. The bindings form a tribofilm which builds up on the sliding surface. When the two surfaces, covered with a boundary layer, are in contact, they tend to slide along their outermost surfaces [Ahmed and Nassar (2013)].

In such a situation, liquid is not the best boundary lubricant. Rather, the best boundary lubricants are solids with long chains of high inter-chain attraction. These chains produce low shear resistance. Hence, they tend to slip easily and can tolerate high temperature.

What differentiates types of lubricants is actually the ability of the lubricant to act as it is supposed to be. Prior research explains that the term ‘lubricating oil’ is generally used to include all lubricating materials that work as fluids. According to Pirro and Wessol (2001), Spikes (2001), Stachowiak and Bachelor (2001), and Pawlak (2003), lubricating oils are made from the more viscous portion of crude oil. This portion is the remainder product after removal by distillation of the gas oil and lighter fraction. As crude oil may vary according to its source, there are relatively small differences in its component analysis. The complexity of the lubricating oil can be considered through variations such as: paraffinic components, naphthenic components, aromatic components and non-hydrocarbon components.

Regarding to the issues raised previously, there were demands in reducing or eliminating the friction. To do so, one needs to understand the mechanism between the contacting surface and what actually happened. According to Findik (2003), we need to understand the driving force that will determine whether friction is preferred or not. In several cases such as bearings, gears, and piston, low friction was preferred meanwhile for brakes, tires, and clutches, high friction were preferred. However, unfortunately for both cases low wear rate were preferred. In order to rely on a machine to work, steady, reproducible, and expected friction and wear value are important for competently and consistently purposes.

It is crucial to understand the fundamental parameters in a lubrication system to determine the reliability of an operation. According to Paszkowski (2013), in bearings, it is crucial to select a suitable type of lubricant that ought to reduce coefficient of friction and wear. Those lubricants also are required to protect the components from corrosion and erosion. Wrong type of lubricant may lead to higher operating and servicing cost.

It is generally noted that rolling possessed much lower friction resistance than sliding. That is the reason why rolling application were most used such as wheels and bearings. Findik (2003) explained that rolling friction is generally incredibly small. It may be achieved through inelastic deformation in the material. The hypothesis is the bigger the hysteresis loop, the bigger the energy loss hence it lead to smaller coefficient of friction. That is why rolling is chosen as bearing's operating method.

In most machines, bearing are one of the primary components. Bearings are not simply reducing the friction resistance and wear but it also supporting the weight of rotor and influencing the dynamic behaviour. According to Pai and Hargreaves (2000), since Egyptian Empire lubricated journal bearing had been used; in this case by using animal fats. This concept had been accepted widely and lead to the industrial revolution. Relative to the population on earth, it is wise to say that the number of journal bearing are exceeding the human population on earth.

Technically, bearing act by rolling two or more cylindrical (for journal bearing) and sphere (for ball bearing). In order to reduce more friction and wear, lubricant were introduced between those cylindrical/sphere surfaces. As results, the wear reduced drastically due to the reduction of friction and heat dissipated.

The common aim of bearing is to ensure a good hydrodynamic lubrication system when operating besides avoiding contact with the shaft. Commonly, oil were used in bearings, however other liquids are also possible such as water. Although the viscosity of water is a lot lesser, but under certain circumstances, it is applicable. Besides water, semi-solid such as grease can also be used.

Recently, the increasing in ecological awareness had become a crucial element in the law for environmental protection. According to Pai and Hargreaves (2000) current oil lubrication has many disadvantages such as:

a) Oil-based lubrications are hazardous to the environment.
b) Many systems such as turbine require cooling system.
c) Requires complex sealing system.

Regarding to that matter, several solutions had been proposed by researcher such as Abdollah (2013), Ahmed and Nassar (2013), and Pai and Hargreaves (2000)to create a different type of lubrication in bearing. Unfortunately, those ideas are still insufficient to replace current oil-based bearing completely. But somehow it is still a better solution towards this problem. Those solutions proposed are including water-based (liquid), nitrogen (gas), and self-lubricating (solid) bearings.

2.2.1 Water lubrication

Water lubricated bearings consist of cylindrical shell and liner. According to Pai and Hargreaves (2000), the bearings are made from hard plastics through casting and rubber. They also add that rubber and water is a perfect combination system for bearings. Due to rubber's unique natural properties, it provide a good absorption of vibration, noise, and also impact towards the system. Pai and Hargreaves (2000) also explained that a layer of water were created between the shaft and bearing during rotation. They explained that the waters enters the bearings through the longitudinal grooves and moves radially between the contacting surfaces in a thin film.

This film is actually becoming the boundary between the two contacting surfaces. The constant flow of water leads to wear reduction due to lower friction and heat generated. This such technology were implies in marine application such as in boats and ships.

2.2.2 Gas lubrication

Ahmed and Nassar (2013) explained that gas lubricated bearings are the simplest and lowest viscosity type of bearing's lubricant. This type of lubricant is mainly applied in aerospace industries. Due to constant chemical properties over different ranges of temperature, gas lubricant provides several advantages over other type of lubricants such it is applicable at extremely low and high temperatures. Gas lubricant also eliminates any contaminations' risk in food and pharmaceutical industries.

According to Abdollah et al. (2013) whom synthesis previous study such as Cong et al. (2000) and Martin et al. (1990) stated that gas bearings are applicable for extremely large surface velocities. Abdollah et al. (2013) also explained that several research before they had stated that gas lubrication can lower the friction at high load, sliding speed, and distance.

This simple were because of the shear strength that increasing is less proportional to bigger applied load, speed, and distance.

In the study by Abdollah et al. (2013), they compare a friction coefficient and wear between oxygen and nitrogen lubrication using four ball tester machine. They found that nitrogen provided better lubrication purposes compare to oxygen. They proudly stated that nitrogen gas present lower friction coefficient by 24% with smaller diameter scar compare to oxygen.

2.2.3 Solid lubricants

Generally, solid lubricants were solid materials that is implemented as a coating film between two contacting surfaces. In other words, suitable and adequate solid were applied on one surface before contacting with another surface. Regardless, solid lubricants are used to reduce friction and wear just like other lubricants. According to Ahmed and Nassar (2013), solid lubricants were usually used under extremes operating conditions such as at a critical temperatures and corrosive environment. They also added that solid lubricants normally have a structure like crystalline layers that actually works as friction reduction agent.

The most applicable solid lubricant nowadays is Diamond like Carbon (DLC). The DLC is in a form of carbon coatings on the contacting surface. The DLC can possess low friction coefficient and wear compared with other lubrication systems. Detail discussion regarding DLC will be discussed on the next subchapter.

Ahmed and Nassar (2013) stated that self-lubricating materials are particularly important to bearings technology. Self-lubricating materials is generally a material that able to produce its own lubrication without any external lubrication feed. Their unique characteristics will eliminate the dependability of oil, gas, or grease and also improving the bearing's performance at high temperature. Ahmed and Nassar (2013) also add that graphalloy (graphite/alloys) possessed a special properties of graphite where it can appear almost like the DLC structure while maintaining its independent ability towards lubrication.

This kind of lubrication is emerging in tribological fields due to its potential as an efficient friction and wear reduction agent. Detail discussion on self-lubricating materials will be discussed in the next sub-chapter.

Besides graphalloy concept, friction and wear agent were also studied based on polymer composite perspectives. Previous study by Rymuza (2007) synthesises several studies and explained that the Tribology of polymer-to-polymer sliding are somehow promising but yet the knowledge are still very limited. Among the polymer group, the most popular polymer type selected were thermoplastics. This is because thermoplastic composites are easier to cast compared to thermoset. However, the ultimate disadvantages of thermoplastics is it is very dependable to temperature.

2.3 Self-lubricating Materials

Another trend that has caught the eye of researchers nowadays in the tribological domain is the application of hard coatings. It focuses on potential elements which can exist in various forms such as carbon. Carbon can exist in various forms, such as in sp3 hybridisation (as diamonds) and in sp2 hybridisation (as graphite). Carbon also exists in amorphous form (e.g., as fiber, soot, glassy carbon).

At present, there is very little published information available on the mechanics of friction and wear of self-lubricating composites containing soft second-phase particles. Historically, the first attempts to investigate self-lubricating materials were made in Russia during the 1970s.

Nosonovsky and Mortazavi (2012), in their book, summarised the observations of a previous research that friction and wear are from the same phenomenon and have the tendency of energy to attain a certain state. However, it can also lead to various mechanisms and sometimes causing self-organisation of the secondary structures. This structure is called 'nonstoichiometric and metastable phases'.

The friction force is also a reaction on the informational (entropic) excitations. This reaction is analogous to the elastic properties of a polymer, which mostly related to the change of entropy. This reaction also have the magnitude of the order of the elasticity of a gas. Self-lubrication refers not only to coatings, but also to the development of metal-, polymer-, or ceramic-based composites. These types of composites often provide structural integrity and as a reinforcement material which can present low friction and wear.

Studies have shown that the COF in these self-lubricating materials is related to the formation of interfacial films, often called as third body or tribofilms. Due to the interaction between the asperities during the sliding, a plastic deformation occurs, forming a film layer.

According to Alexeyev and Jahanmir (1993), the formation of a soft transfer film is triggered by the deformation between the matrix and the soft phases. In this case, the matrix were harder element that released through breakage. Then, with the release of the debris towards the surface, the debris spreads on the surface, forming a thin lubricating film, as illustrated in Figure 2.3. If the tribofilm is not affected by wear, the thickness of the film is controlled by the plastic deformation.

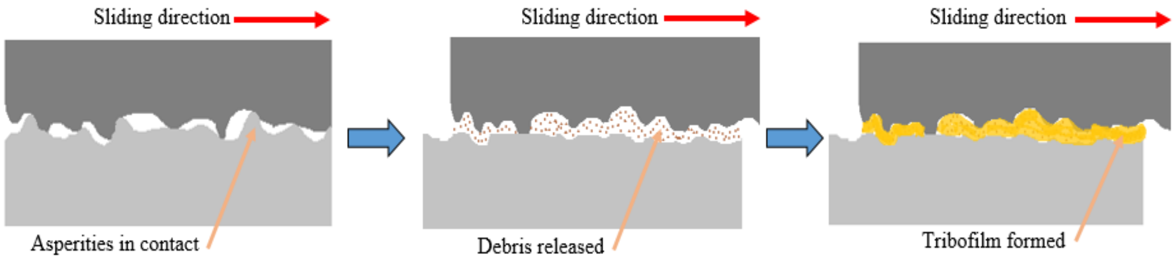

Figure 2.3 Flow of tribofilm formation
[Source: Ludema (1996)]

Tribofilms can be divided according to their process of generation, which involve complex mechanical, chemical, and thermal reactions. Biswas (2000) discussed three types of tribofilms formed in metal-to-metal and metal-to-ceramic sliding interactions. These are mechanically mixed, chemically generated, and thermally activated tribofilms. Luo (2013) stated that tribofilms can be grouped into:

a) Tribofilms generated from the wear of the main event of the sliding couple surfaces;
b) Tribofilms generated from the resulting wear of the soft material; and
c) Tribofilms generated as a result of chemical reactions between the wear products and the environmental species.

These days, polymers are a very promising substance to be used for self-lubricating materials in components, machines, and devices. However, not all polymers are able to do so. By understanding the friction and wear mechanism, some are able to estimate and recreate a self-lubricating material that has the potential to become a low-cost, corrosion-resistant substance, with vibration damping, and having the ability to adapt to work in the presence of contamination, among other advantages. These include the potentials in sliding and rolling [Ryumuza (2007)].

Polymeric self-lubricating materials can operate without lubrication and have wide potentials to be modified by adding fillers, lubricants, and additives (Brostow et al. 2010). Thus, these materials can offer great perspectives to create self-lubricating polymer composites that possess excellent tribological properties.

A study by Chua et al. (2013) showed that COF and wear rate can be decreased with the application of polymer composites by reinforcing them with some activated carbon. They found that as the load increased, the COF and wear rate decreased. Due to the increase in frictional heating, a tribofilm was formed, as adhesive and abrasive wear were traced. However, the authors also found that the tribofilm was broken at higher load.

Natural fiber reinforcing aluminium, too, has become one of the attractions of study in the tribological field today. Much research such as Debnath et al. (2013), Bakry et al. (2013), Nirmal et al. (2015), and Zamri and Jamaludin (2011) has been done internationally and domestically on substituting natural fiber, ash, and particles into a metal matrix, which has shown promising potential in this field. However, there are more gaps that can be filled within this area.

In comparison to ceramic or metallic, self-lubricating materials are easier to be constructed through polymer. Hence, it can be said that the technology of polymer is important for future development in the Tribology field. The study presented above showed that polymers have potential as tribological materials as they are very good as low-cost, self-lubricating materials.

2.4 Wear Modes

The transfer of element between two contacting surfaces are called wear. Normally, wear occur as accompany to friction. There were three conditions that can cause wear:

a) Surface to surface contact

b) Surface with foreign/alien substances

c) Erosion through high speed or corrosion

Adhesive wear usually happened when two contacting surface contact and as a results, the wear particles (debris) of softer surface stick/glued at harder surface. Abrasive wear is type of wear where asperities of the softer surface got cut and release as wear particles by harder surface. Corrosion occurs when there were oxide layer present in between two contacting surfaces. The oxide layer then were weakened the surface and released as corrosion products. Also, erosion occurs when there were impact from high speed sources such air or water resulting to releasing a clump of debris into the air. The illustration of the mentioned type of wear were illustrates in Figure 2.4.

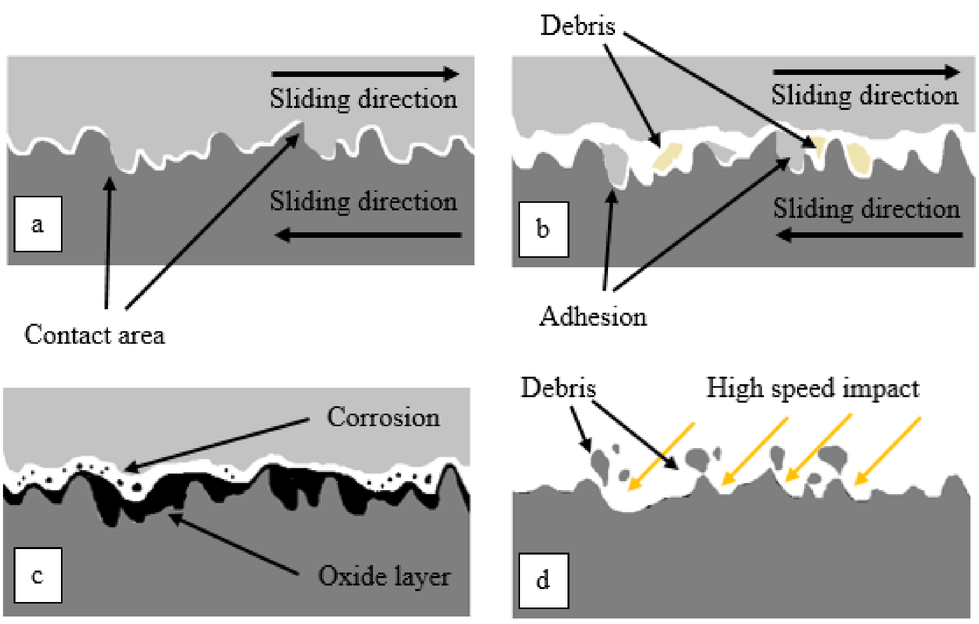

Figure 2.4 Illustration of (a) contacted peak between surfaces, (b) adhesion and abrasion wear, (c) corrosion, (d) erosion

According to Sinmazcelik and Taskiran (2007), wear usually changes through three different stages, which are primary, secondary, and tertiary stage.

a) Primary stage: occur during “running in” period. At this stage, the contacting surface is trying to adapt with the asperities between the surfaces. As a result, the wear rate are not constant and may vary.

b) Secondary stage: occur during constant wear rate period. In this stage, the surface has already adapts with the asperities. During this stage also the abrasive and adhesive wear usually occur.

This stage is usually varies depending on the environmental conditions such as temperatures, velocities, loads, and many more.

c) Tertiary stage: occur when the components fail.

The stages were illustrated in Figure 2.5 below.

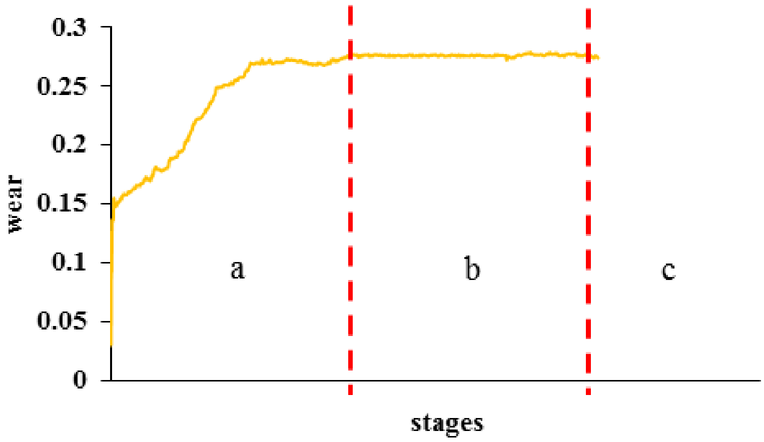

Figure 2.5 Illustration of wear stages

By the explanation of Treutler (2005), he found that there were two types of wear modes in the DLC coatings under repeated impacts. The first mode were the interface failure and the second mode were cohesive failure mode (fatigue).

Meanwhile Kapoor and Franklin (2000) found that the failure of tribolayer of ductile materials also occurs at two different dependent mode, which are cyclic strain and also low cycle fatigue.

Terrel et al. (2012) discussed report by Kotzalas and Doll (2010), there were several modes that occur in wind turbine bearings. The most common modes fatigue due to rolling contact. It is mainly due to relatively high stress. This stress produced cracks under the surface which then will propagate to the surface. Also, fretting wear is also common that it occurs within bearings for wind turbine. According to American Gear Manufacturer's Association (2004), this problem occurs when the turbine was shut down for maintenance, the low amplitude motion due to wind gusts.

2.5 Tribological Effects on Metal Matrix Composites

Metal matrix composites (MMC) have been used in the aerospace, aircraft, and automotive industries because they possess many potential advantages over monolithic materials, such as higher specific strength and stiffness, higher wear resistance, higher thermal conductivity, and lower coefficient of thermal expansion. When solid lubricants such as graphite are introduced at the sliding interfaces, the friction and wear noticeably decreased.

Graphite consists of carbon atoms which are arranged in a layer-like structure, and produces very low COF (0.1–0.2). Hence, researchers suggested on using graphite as a solid lubricant. Donnet and Erdemir (2004) reported that graphite is an effective lubricant additive because it is anti-corrosive, and has high temperature endurance and self-lubricating properties produced from its lamellar structure. The gap between lamellar materials produces excellent lubricating properties under heavy loads.

Just like other materials, graphite also has its drawbacks. One of the major problems in using graphite as a solid lubricant pertains on how to maintain a continuous supply of graphite between two sliding surfaces. A continuous supply of graphite is more easily maintained in fluid lubricants compared to solid lubricants. Thus, much research has been conducted on generating ideas for incorporating graphite into a metal matrix composite. One of the ideas was creating self-lubricating composites which contain solid lubricants such as graphite.

Since wear is a cyclic motion phenomenon, the debris that was released during sliding will get stuck between the two contacting surfaces. Hence, implementing the self-lubricating idea is almost based on the same concept. These wear particles, acting as a third body formed at the interface, function as solid lubricants and decrease the friction coefficient and wear rate.

Under dry sliding condition, Zamri and Shamsul (2011) explained that metal-graphite composite turns self-lubricating because of the transfer of the graphite that adheres to the asperities of the harder surface and forms a thin film of graphite. This thin film prevents direct contact between the contacting surfaces. This film reduces frictions and wear. Hence, it can eliminate the use of external lubricants.

Zamri and Shamsul (2011) noted that the content of carbon in the MMC has an effect on the wear rate of the MMC. The PSAC particles used were in the irregular shape of ashes. They found that the cumulative wear rate of the samples decrease with the addition PSAC content at less than 10 wt.%, however, after 10%, the wear rate starts to increased.

Figure 2.6 shows their findings. Smaller pores were found in lower carbon composition and a high pores interface was found at higher carbon composition.

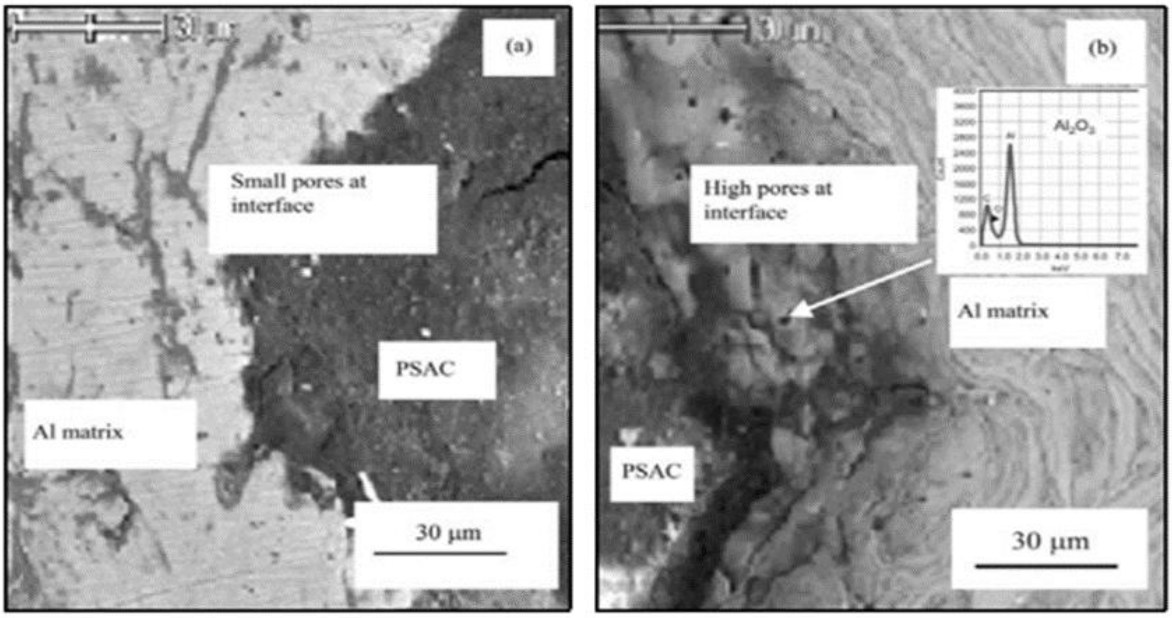

Figure 2.6 Interface between Al matrix and PSAC at (a) 10% of PSAC composition and (b) 20 of PSAC composition
[Source: Zamri and Shamsul (2011)]

A metal matrix graphite particle composite combines the properties from the metal component and mix with the graphite behaviour. Thus, it delivers better strength, hardness, and abrasion resistance. Earlier, metal matrix composite was formed using the powder metallurgy (PM) method as it is easier, cheaper, and can save more material.

Akhlaghi (2009) explained that in metal matrix composites, the tribological properties improve the composite through the formation of a graphite-rich film on the tribosurface, which provides solid lubrication. This tribofilm is formed as a result of shearing graphite particles that are stuck between the sliding surface of the composite. This tribofilm helps decrease the magnitude of the shear stress transferred to the material between the contact areas and reduces the plastic deformation in the contact region. Thus, it helps in the reduction of friction and wear.

As the graphite content increases, the wear rate becomes lower due to the formation of the tribolayer. This is because graphite's particle act as layer that prevent from the two surfaces contacting with each other. In other words, the graphite cause third body contact which the third body will mingle and rolled along the asperities. This concept has been proven in earlier works by Akhlagi (2009) and Rohatgi (1992). Other researchers too had observed that when graphite particulate was released, it helped in reducing the friction coefficient and increased the damage resistance quality, thus improving the tribological behaviour of its base alloy.

Donnet and Erdemir (2004) rephrased other works pertaining to observation of friction and wear behaviour. They observed two major stages as follows:

a) Transient state – a state where the graphite film is still being manufactured, and

b) Steady state – a state where the graphite film has been formed.

2.6 Tribological Effects on Polymer Matrix Composites

Polymer is a large molecule composed of repeating units. Polymers are divided into two major groups – synthetic and natural. Because polymers can possess such unique properties, their demand has increased recently. Besides its properties, polymer can be produced at a lower cost, is plausible to manufacture, and can be applied in wide areas.

The Tribology of polymer is based on Tribology of metals or MMC. Polymer presents a very low surface-free energy and viscoelastic properties. It usually causes drastic tribological changes such as adhesive wear. Polymers are also easily modified, either on the surface or in bulk. Ryumuza (2007) discussed that polymers are often used as a reinforcing material to produce other composites with a variation of physicochemical properties. This behaviour makes polymers a very potential material that may control their frictional coefficient and wear behaviour.

Polymer-based materials (PBMs) are at advantage and hold potential to replace metals in industries. According to Brostow et al. (2006), the advantages of PBMs are low density (compared to metals), low cost, low maintenance, and energy saving. Certain amount of fuel in cars can be saved as the density of polymers is lower than the density of metals. Also, the application of polymer coatings has been under focus lately, especially carbon nanofibers. Researchers such as Altstädt et al. (2002) also found that carbon nanofibers display an excellent improvement of properties compared to metals.

According to Ryumuza (2007), polymeric materials' properties may change or varies with time due to their viscoelastic behaviour. These behaviour effects in drastic differences when considering adhesive and mechanical components of friction force. This effect was also known as stick-slip effect. Due to these properties, some researchers expect correlation between tribological and mechanical properties as the macroscopic properties of polymers are highly dependable on the molecule structure.

Brostow et al. (2010) synthesised other works stating that polymer has complex structure and behaviour. It can be analysed by using computer simulations. With computer simulation, the advantage is that it can provide information that cannot be contained through experiments. Creating polymer structures are much more complex than the creation of a metal structure. This is because the polymers consist of macromolecular chains that vary in length, orientation, and composition. All this unique behaviour of polymers makes them a huge contributor towards affecting the tribological as well as other properties of polymers.

Polymer-based composites are widely used due to the combination of great mechanical and tribological properties. These properties work even better in dry friction conditions, where lubricants cannot be used. Polymers are usually paired or combined with metal materials. However, it might be advantageous for polymers sliding against polymers rather than against metal materials in some circumstances. This is because polymers are light weight, do not corrode, and can be easily manufactured. However, there are still huge gaps concerning the friction and wear of polymer–polymer combinations (Brostow 2003, Ryumuza 2007).

The friction between polymers can be divided into two main mechanisms – adhesion and deformation. The friction coefficient may rise with the increase of adhesion progress between the two contacting surfaces. Vincent and Zambelli (1998) explained that a polymer on polymer sliding will create adhesion hysteresis. The mentioned adhesion hysteresis is actually a phenomenon where two contact surfaces dissipates more energy than bringing the surfaces together.

Myshkin et al. (2005) explained that the molecular chain of polymer breaks at the surface was an important factor in determining adhesion, adhesion hysteresis, friction, and wear. In addition, frictional heat that occurs between the sliding surfaces will change or at least affect the physical state of the sliding surface. The change also makes a significant contribution towards tribological behaviour under dry sliding conditions. As contrary to PBMs, oil lubricants can reduce or eliminate frictional heat.

The major wear mechanism under dry sliding conditions was adhesive wear. For an oil-lubricated condition, adhesive wear combined with erosion wear was the dominant wear mechanism. A study summarised by Ryumuza (2010) suggests that the dry sliding of polymer on polymer surface produces stick–slip motion due to adhesion. They also found out that the sliding combination of two rough surfaces shows lower COF compared to sliding of two smooth surfaces.

The concept of polymer to non-polymer contact is often applied in various machines and devices. Previous research has attributed this to the good mechanical and thermal properties between the two contacting surfaces. The typical tribological combination is steel to polymer surface contact. A relatively low friction coefficient and often sufficiently high wear resistance can be achieved. The two main components of polymer and non-polymer contact are adhesive wear and its mechanical properties.

The mechanical properties and adhesive interactions can be found at the thin surface layer of the polymer that is in contact. The COF is usually very high at low surface roughness because of high adhesion, and minimum at higher surface roughness. The COF increases for a further rougher surface when the mechanical component of the friction force becomes very high. A similar pattern was also experimentally proofed for the wear rate. When the load increases, the COF decreases. However, this only happened at elastic boundaries. When the plastic deformation begins, the COF is relatively low but it increases due to addition of load. The sliding speed and temperature have a significant effect on this type of contact. For polymers with higher glass transition temperature, the maximum value of friction coefficient appears at higher sliding speed.

Adhesive and abrasive wear mechanisms often occur in many sliding systems. The wear rate is high at a high contact pressure and sliding speed. At a higher condition, the friction is controlled by the transfer of materials. This phenomenon is the most important role in the friction and wear of PBMs. The process of transferring polymer material on to the non-polymer material is usually initiated by local adhesive bonds between the rubbing surfaces. Transfer film is very important, especially under dry friction condition. The transfer film formed is controlled by the properties of material and surface roughness, and sometimes, sliding conditions.

The tribological condition of polymer generally improves during the friction process. This results into lower COF and significantly lower wear. PTFE-based composite is one of the examples of this situation. However, the inter-relation between the transfer film layers and the adhesion between the transfer film and the counter surface is still lacking in general. The material transfer is very important in the Tribo-study. This is where polymer composites are very popular as materials for sliding components. Sliding components mentioned here pointing to materials that often suggested to reduce friction. This is because, according to Ryumuza (2007), the reinforcing of fibers or powders of solid lubricant can change the physical properties of the composite drastically, especially in both friction and wear behaviours. Some refinements may enhance the adhesion of polymers.

Another crucial property is mechanical behaviour. The thermal conductivity and lubricity may reflex to further development of this material's potential. The complex structure results in a complex behaviour of the polymeric tribosystem. Metallic, ceramic, and metal oxide is added to polymers with the expectation to obtain some unique and positive mechanical properties.

Nano-scale studies in the tribological field focused on polymers are gaining significance. This is because the potential of polymer as a material in the nano system is plausible. The tribological behaviour of polymer is important in various fields such as nano-imprint lithography.

Static and dynamic friction depends on the interface of materials. These may occur in terms of contact, chemical reaction, thermal reaction, surface profile, humidity, and presence of lubricants. All this may change through chemical and other methods, thus affecting the friction behaviour. The contact surface of pure metals and alloys contains something called metallic bonds, which creates a strong adhesion and hence may increase the friction and wear.

Brostow et al. (2010) stated that metal oxides and other foreign objects may lower the adhesion, and hence the friction. Some other materials such as ceramics were used in extreme conditions due to their high mechanical strength and resistance. This behaviour was formed due to its strong ionic bonds at room temperature. Lower friction compared to metals was noted. Generally, polymer possesses low stiffness and strength. Hence, it exhibits low frictions due to its weaker interactions but higher wear. Thus, to balance between a good mechanical strength with low friction and wear, polymer composites were necessary.

Lubricants used in the forms of powder, solids, or oil generally can reduce friction by creating a film on the contact surface. To create a protection against wear and to reduce friction, lubricants were applied. However, this idea only idealised to metals and ceramics. Generally, polymers, on contacting with liquid lubricants, will swell. The transfer of mechanical energy can affect its bulk energy. This transfer will cause interactions at the interface, affecting the friction and wear. Thus, the physical and chemical nature of the surface of the contacted materials and also the surface topography might change.

During friction, the heat that is generated can cause wear through mechanical or chemical or both. Wear mechanism can be fatigue, adhesion, abrasion, erosion, and corrosion. Sometimes, there are circumstances where there is no presence of a single mechanism wear, but rather a combination of those mechanisms. The breaking of bonds between actual contact surfaces can control some adhesive wear component. Brostow (2010) cited a previous study by Buckley (1981) that Van der Waals interactions and hydrogen bonds are usually present for most polymers. Interfacial bonds may break through the shearing of asperities during the movements. Harder surfaces or asperities cut or plough the softer surface. The cutting points are called debris. There were two conditions where abrasion occurs – when the debris are released in the contact area or embedded in the counter face. They were termed three-body abrasion and two-body abrasion.

The adhesive wear process goes from creation of adhesive bonds, their growth, and breaking. Under certain circumstances, the wear usually is not the products of a single mechanism but rather product of a combination of different mechanisms. Generally, wear is often categorised as the unwanted loss of solid materials caused by mechanical interactions.

According to Brostow (2010), wear is determined from the volume loss during the sliding interactions. However, he also argued that it cannot give reliable results because the amount of debris stuck and dissipated to the environment depends on the sliding speed of the two contacting surfaces.

It is generally known that as sliding creates energy due to friction, heat is also generated. This is because the contact between two surfaces due to friction generates movements between elements that causes energy released through the breakage of Van Der Wall bond. This energy released were in the form of heat (thermal energy). Hence, higher speed will produce more heat.

2.6.1 Tribological Effects on Polytetrafluoroethylene

Polytetrafluoroethylene (PTFE) polymer is widely used in high performance mechanical seals. Previous studies explain that it is due to its high chemical resistivity, low COF and high temperature stability. Lancaster (1990) reported that the friction between polymers can result into two main mechanism defects, which are deformation and adhesion. Through deformation, the mechanisms involved are in complete dissipation of energy within the contact area. Meanwhile, the adhesion component is responsible for most of the friction of the polymer. These are the results of the breaking of weak bonding forces between polymer chains of the material and the transfer film.

Unal et al. (2006) reviewed previous research in related fields and concluded that for PTFE polymer, the formation of low shear strength film creates low COF during sliding. Unfortunately, this film forms at a high rate, and hence, produces low wear resistance. This behaviour results in leakage problems in seals application. According to Brisco (1981) and Watanabe (1992), wear resistance likewise can be improved by the addition of filler materials. Bahadur (1985) and Lu et al. (1996) stated that the addition of fillers is an important component in the formation of transferred films structure, as well as the stability and adhesion between the contacting surfaces. Briefly said, the addition of fillers can reduce wear.

The potential of PTFE as wear resistance material can be improved through the addition of carbon due to the preferential load by the fiber. Studies have also been done with the addition of particulate filler such as graphite to improve PTFE potential. The graphite fiber filler materials—present and stuck with the addition of the fragmentation of the PTFE—create the formation of small discontinuous fragments which reduce wear rate of the composite.

PTFE is also widely used for bearings and sliding applications due to its low COF, high toughness, and high thermal stability. According to Goyal and Yadav (2013) and Rae and Dattelbaum (2004), PTFE also shows good resistance to organic solvents and acids. However, it exhibits a higher wear rate compared to other polymers under dry conditions, and a high orientation of PTFE molecules in the transfer film may be the cause of low COF.

A previous study by Sawyer et al. (2003) found that the wear rate of PTFE nano composites decreases with increasing other filler contents. In contrast to this, Li et al. (2002) reported a slight decrease in the coefficient of friction by increasing ZnO contents. Likewise, the particle size of fillers also affects the wear rate of composites since a huge reduction in wear rate of nano composite is released and results in better interaction between the PTFE matrix and the alumina (Al_2O_3) particles. However, the addition of Al_2O_3 particles into the matrix increases the COF.

High performance mechanical seal is also one of the current findings on PTFE. This is due to its unique properties such as low COF, high temperature stability, and high chemical resistivity. According to Khedkar et al (2002), Blanchet and Kennedy (1991), and Lee (1985), despite these positive potentials, PTFE also possesses poor wear and abrasion resistance. This problem is the main reason for early failures in solving the leakage problem in the seals. However, this problem can be improved through the addition of filler—depending on the type, shape, and size.

Khedkar et al. (2002) compiled a series of studies which confirmed the dominance of carbon-fiber-filled and graphite-filled PTFE. Presently, the need is for more advanced wear resistance materials with a probable addition to the composite to achieve significantly improved lubricating materials. This idea will be credible if a pilot project is conducted which will demonstrate PTFE’s relatively low COF against steel since PTFE has the ability to extend its chain of linear molecules.

Previous research proposed that the addition of carbon fibers to PTFE can improve its wear resistance while others reported on the use of graphite to modify the tribological properties of PTFE. According to these studies, PTFE tends to fracture under heavy loading conditions, and thus cause abrasive wear.

A common denominator of these studies is the recommendation that adding two or more filling materials can result into potential lubricating materials. Hence, it can be concluded that the aspect ratio of materials is an important parameter in manipulating tribological behaviour. Some researchers such as Brostow (2010) find abrasive wear for polymer as rather interesting, although he agreed with Myshkin (2005) that the core of abrasive wear is the cutting and ploughing of the surface by a harder surface, which led him to look into the mathematical implications as well.

Based on this presented argument by Brostow (2010), it can be said that the main problem with polymer-based materials (PBMs) is that PBMs behaviours are strongly dependent on temperature, low thermal conductivity, and high tendency. Briefly, PBMs are sensitive to environmental changes. Besides that, PBMs depends on the composition and thermal history for solidification or the curing process.

2.7 Potential of Amorphous Carbon on Tribology Applications

As mentioned in the previous section, carbon can be found in various forms of hybridisation. Somehow, Grill (1998) found that the relation among graphite, diamond, and also polymer is closely linked with carbon and hydrogen arrangements. Figure 2.5 illustrates what Grill has summarised by referring to Koidi et al. (1991).

Through Figure 2.6, it can be seen that polymers may and can have the potential to be like DLC. However, the gap of knowledge in polymer-based materials is still wide and needs to be studied. From what was discussed in this chapter, it can be concluded that there are several materials which have the significant potential in the field of Tribology. These materials are: diamond-like carbon (DLC), fiber-reinforced polymer (FRP), and carbon fiber-reinforced polymer (CFRP).

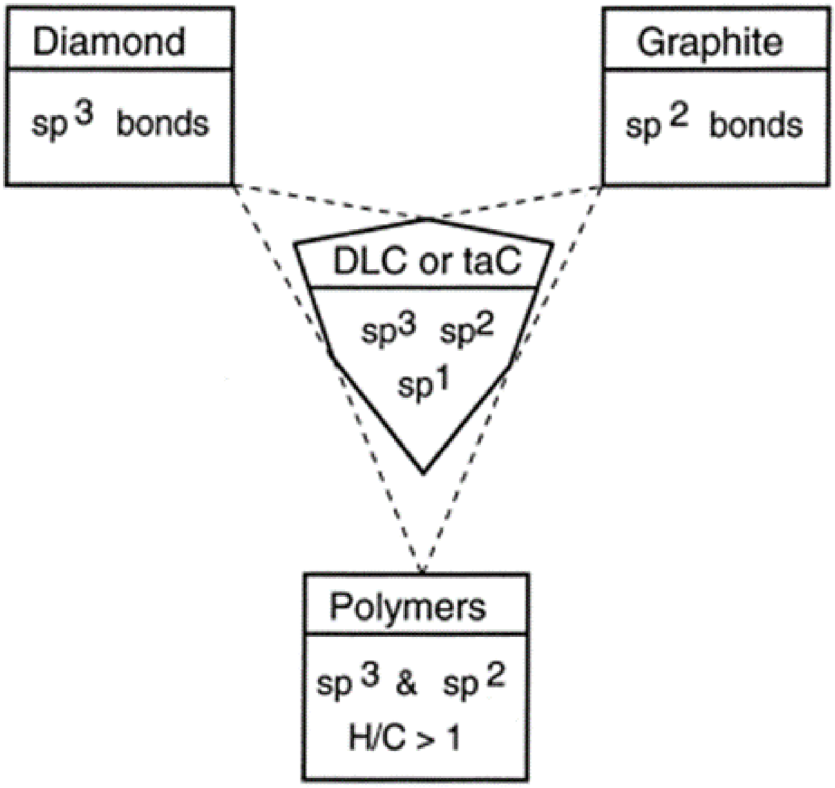

Figure 2.7 Relations among DLC and diamond, graphite, and polymer
[Source: Grill (1998), and Koidi et. al (1991)]

2.7.1 Diamond-like Carbon

Diamond-like carbon (DLC) is a concept where carbon can coexist in sp3 and sp2 in a connecting network and either as amorphous carbon (a-C) or hydrogenated amorphous carbon (a-CH). Kadiayala (2006) stated that diamond has extremely high hardness. Besides, diamond also has good thermal conductivity and chemical inertness. According to previous research such as by Abdollah et al. (2012), diamond has low COF and wear rate. When combining all these characteristics, it shows that diamonds are useful as cutting tools more particularly in high-powered electronic devices.

On the other hand, in contrast to diamond, graphite is very soft. Tribologically, graphite has low COF but relatively high wear, and it is also well known that graphite is a good solid lubricant [Abdollah (2010) and Guy (1976)]. Through their own ability, it is interesting to combine both elements to create potentially good lubrication materials.

Additionally, carbon can be found as diamond, graphite, and amorphous carbon. Diamond-like carbon was raised by Aisenberg in 1971 and now, DLC is commonly used for hard carbon coatings since it has similar properties as diamond, but does not have a crystalline lattice structure. DLC films have received much attention over recent years and have been under intensive research since the middle of the 1980s as DLC presents a broad range of applications that are beneficial to the field of Tribology.

Carbon has three different types of bonding configurations, which are sp3, sp2, and sp1. The bonding of DLC and graphite is illustrated in Figure 2.7. According to Guy (1976) and Bushan (1999), carbon has four sp3 hybridised orbitals in diamonds. These sp3 orbital forms four equal carbon-carbon bonds that produce the tetrahedral structure of the diamond. This tetrahedral structure is the cause of high hardness and high thermal conductivity of carbon.

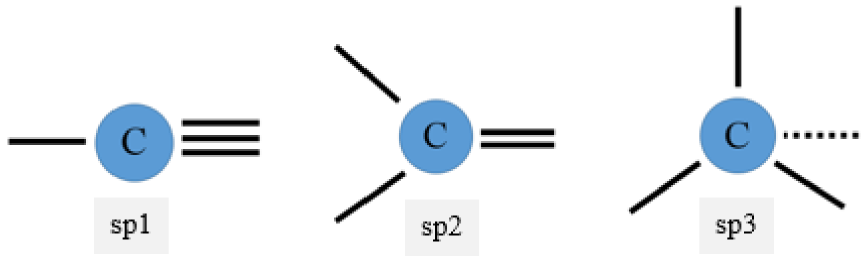

Figure 2.8 Atom configuration of sp1, sp2, and sp3 carbon

On the other hand, unlike diamonds, graphite has three tri-gonally plane sp2 hybrid orbitals [Abdollah (2011)]. Each carbon atom in the plane is bound with strong covalent bonds [Kadiyala (2006)]. However, the layers of carbon atoms are only bound by weak Van der Wall's forces. This phenomenon is the producer of the layered structure of graphite. The layers can break easily, which accounts for the low friction property of graphite. These bonding configurations are illustrated in Figure 2.8.

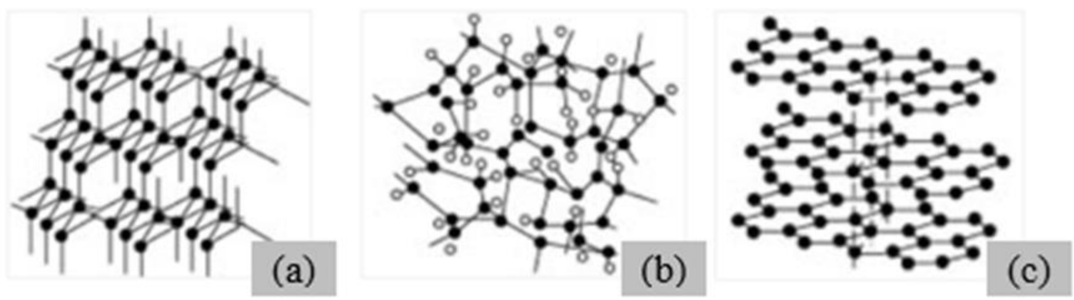

Figure 2.9 Atomic bonding of (a) diamond, (b) DLC, and (c) graphite
[Source: Guy (1976)]

DLC film has been used as coating materials. By altering the properties of the element, DLC may vary in aspects of friction, wear, corrosion, and many more. Although DLC is used widely, there are certain limitations on what DLC can perform. According to Grill (1999), some of the limitations of DLC are low toughness, poor adhesive materials, and high internal stress.

Grill (1999) and Wei et al. (1998) stated that DLC film requires a very smooth surface in order for it to be used as protective coatings for magnetic media, biological implants, and microelectronic applications. Some applications require adhesive ability in order to be functional. For instance, the magnetic recording industry requires crucially thin—about 2 nm—and smooth protective coatings. In addition, the smooth coatings has very low COF.

Liu et al. (1996) showed evidence that the transfer layer contained a fine distribution of graphite nanoparticles in a distorted diamond-like structure. Moreover, the graphite forming process takes place in the wear track region from repeated sliding. Consequently, low shear strength between the two contacting surface is related to the formation of the tribolayer and causes low wear rates.

Erdemir and Donnet (2001) confirmed that both friction and wear of DLC are the results of lubricating effects that form on the contacting surface. On the other hand, rather than frictional heating effect, Voevodin et al. (1996) believed that phase transition from sp3 to sp2 is induced by the stress from the contacts between the surfaces. Hence, Zhou et al. (2005) stated that it is complicated to distinguish if the interaction between two contacting surface is due to physical or chemical interactions.

Regarding this problem, Tabor (1984) discussed the possible solution through a wear map. Subsequently, Abdollah et al. (2012) proposed the development of deformation-wear transition map as a way to study and predict the transition from deformation to wear.

CHAPTER 3

METHODOLOGY

3.1 Experimental Flow

This project focused on finding the tribological properties of PKAC-E using the dry sliding method or the pin-on-disc test. To achieve the discussed objectives mentioned earlier in Chapter 1, the experiment was divided into four phases. The graphical flow of this experiment is shown in Figure 3.1.

Phase 1 started with the preparation of the materials. Particularly, this involved designing the mould, which was based on the required sample size according to the available pin holder size. Having constructed the mould, the PKAC was crushed and sieved. The resulting fine PKAC was mixed with liquid epoxy and compressed. After the black sample or pin was taken out, the sample was set aside for curing before mechanical tests were conducted.

For Phase 2, two types of tests were conducted: standard method testing and arrays based arrangement testing. The standard method tests were conducted at different sliding distances and temperatures. Meanwhile, by using the Minitab software, sixteen orthogonal arrays (L16) were created at different composition, applied load, sliding speed, surface roughness, and temperature. In this phase, the sample was first grinded in sand paper and weighed. Then, the pin was taken to the pin-on-disc machine to be tested. After the dry sliding test, the pin was again reweighed.

In Phase 3, the results collected were analysed. The first analysis conducted was quantitative analysis through calculation of coefficient of friction and wear rate. Then, from the L16 orthogonal arrays results, friction wear equation was proposed using ANOVA. Since the results obtained were statistically accepted—if otherwise, Phase 3 needed to be repeated—the process proceeded to Phase 4.

In Phase 4, the worn surface of the pin was taken to the scanning electron microscope (SEM) and energy dispersive X-ray (EDX) for surface morphological conditions.

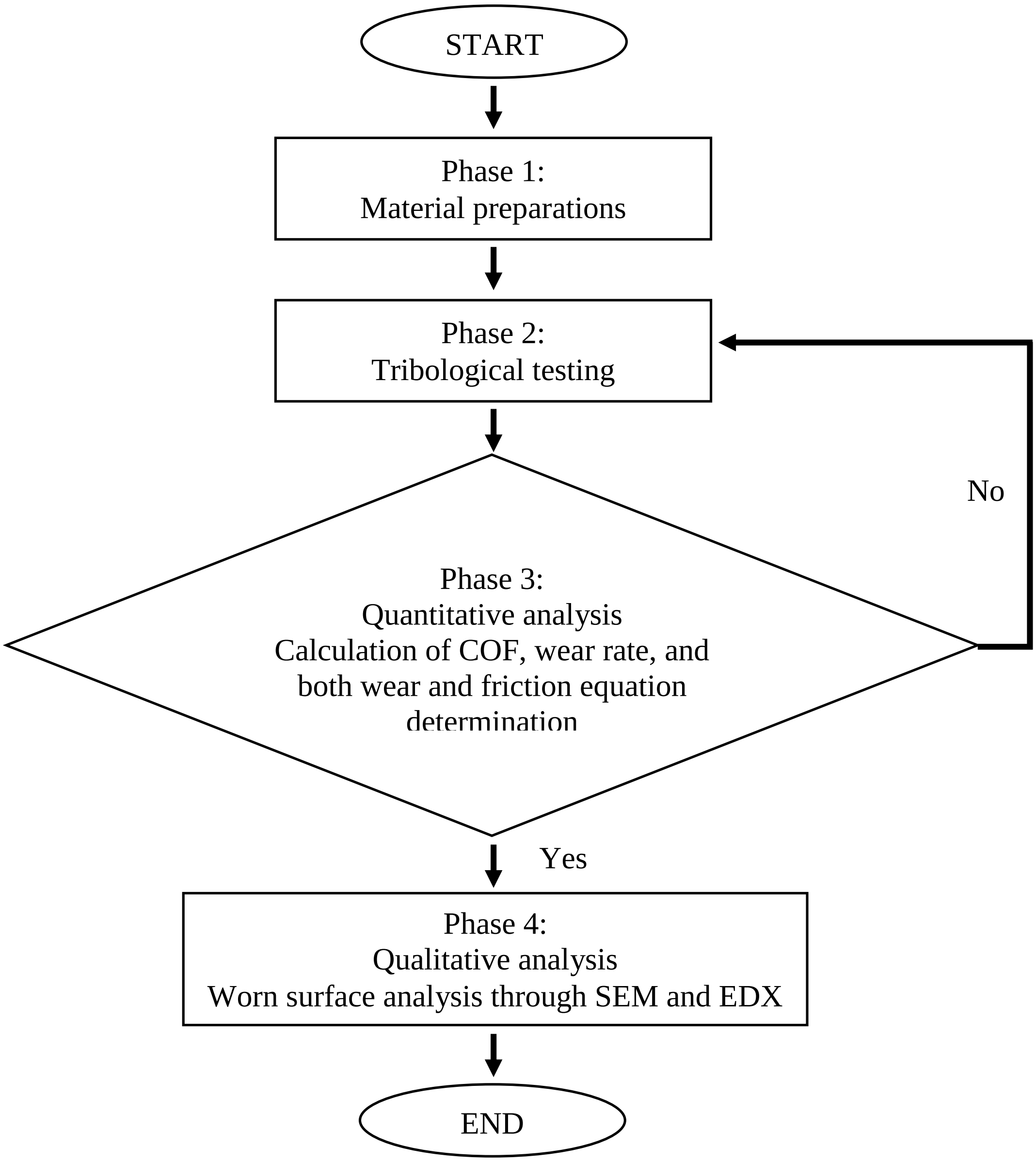

Figure 3.1 Experiment flowchart

3.2 Materials and Sample Preparation

The main materials used in this study were palm kernel activated carbon (PKAC). The PKAC generated from the supplier was still big in size and was not yet suitable for forming using compaction technique. Hence, the PKAC was crushed into almost powdered-like form using a blender and then were sieves using 1 mm size sieves. The remaining PKAC were re-crushed again and re-sieved. The purpose of the sieving process was to ensure that the size of the PKAC used in this study was in a specific range, and additionally, to eliminate any plausible error related to grain size. The microscopic image of the sieved PKAC is shown in Figure 3.2.

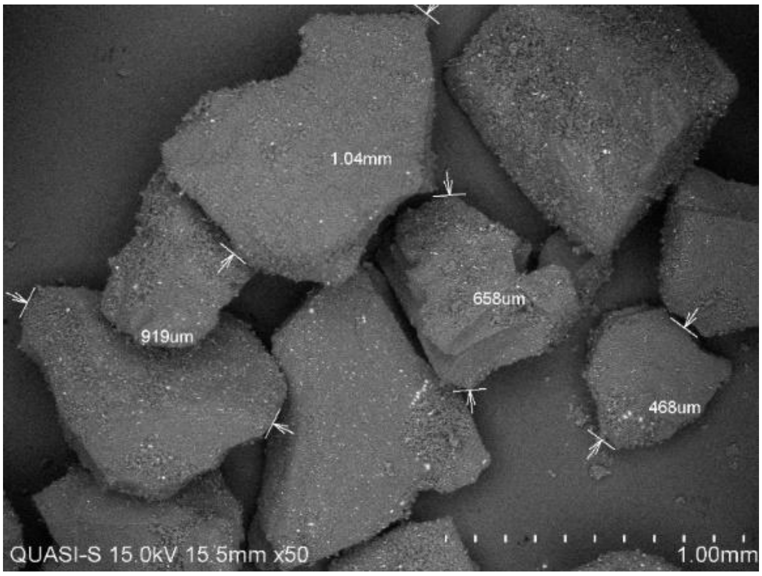

Figure 3.2 Microscopic image of PKAC

Another principal material used in this study was liquid epoxy, particularly a high density epoxy supplied by West System – 105 resin and 206 hardener. Epoxy is in a thermoset group. The reason why epoxy were chosen is simply because epoxy is easier to be handled in liquid form at room temperature compare to other binders.

To solidify, the epoxy resin was mixed with its hardener under suggested ratios by the suppliers in this case, four ratio of resin with one ratio of hardener; that is, the hardening time for this epoxy depended on the ratios between the resin and hardener. In other word, the bigger the differences between the ratios, the longer it will take for the epoxy to harden. The mechanical properties for both PKAC and epoxy used are shown in Table 3.1.

Table 3.1 Mechanical Properties of PKAC and Epoxy (E)

Materials	PKAC	Epoxy (105/206)
Density (g/mm3)	0.42-0.52	1.18
Hardness (GPa)	5 x 10^{-4} - 15.69	7.16
Condition	Solid (1.5 mm max.)	Liquid

To form the PKAC-E into a solid pin, the hot compression technique was chosen since it is one of the simplest and cheapest methods. To compress the solid PKAC with liquid epoxy, a suitable size mould was needed. Hence, a mould needed to be designed. The mould design referred to the desired pin size and availability of the size of hot compression machine. The designed mould is shown in Appendix A.

First, the mould was cleaned thoroughly before the internal area of the mould was wiped with multi-purpose or mould releaser wax. It should be noted that the presence of wax prevents the compressed composite from getting stuck inside the mould.

To form a composite material, it is important to know the basic composition of the composite throughout the process. In composite, there were two main components that need to be accounted for, which are; matrices and reinforcements. Matrices is the main elements in forms of organic or in this case, non-organic (epoxy). The reinforcements may be in the forms of fibers, tubes, or in this case ashes (PKAC).

There were no ASTM standards in producing a composite. Since the composite were done manually based through hand mixing, the calculation of weight distribution were done by referring to Equation 3.1, the composition of the composite determined the weight of the material. After several trial and error process attempts with a 10 mm diameter with 30 ± 2 mm height composite, the weight of the composite was found to be around 3.2 to 3.35 g (for PKAC 60 wt%–75 wt%). The weight composition calculated is shown in Table 3.2.

$$\sum W_{composite} = w_{matrix} + w_{reinforce} \tag{3.1}$$

Table 3.2 Calculated weight of PKAC and Epoxy

W_{pin} (g)	PKAC		Epoxy	
	Composition %	Weight (g)	Composition %	Weight (g)
3.35	60	2.01	40	1.34
3.30	65	2.145	35	1.16
3.25	70	2.275	30	0.98
3.20	75	2.4	25	0.80

The only available clamp that can be connected to the heater were only in the size of 10 mm diameter. Hence, the pin needs to be formed based on that size. Besides, the height of the pin was selected to be 30 mm in the counting of the distance between the disc and the clamp.

Since the amount of PKAC and epoxy was too small, the mixing process was done manually in a beaker and stirred using a spatula. Moreover, it is impossible to mix the materials in large batches because the composite needed to be pressed one at a time, and hence, in the meantime, the remaining composite might harden.

At any rate, the mixed epoxy was then poured into the waxed mould and the mould was then pressed using the static hot press machine after which the mould was taken out and disassembled to extract the sample. Finally, the sample was left for curing at room temperature for one week. The composite were now called PKAC-E composite since epoxy ere synthesised with the PKAC at the earlier mentioned process. The image of PKAC-E composite is shown Figure 3.3.

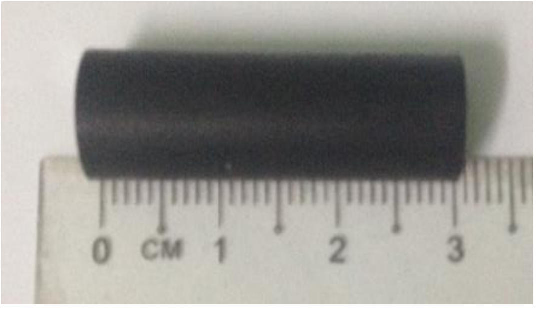

Figure 3.3 PKAC-E composite

During the forming process, several samples were created and tested for the best operating time. Each process was repeated three times to eliminate any human error. The tabulated process is shown in Table 3.3. After selecting the most suitable operations, samples were created. The mould needed to be cleaned and re-waxed after each sample was formed.

Table 3.3 Observation from Heating and Cooling process

PKAC composition (%)	Heating time (min)	Cooling time (min)	Observation
60	5	5	break
	5	10	crack
	10	10	solid
	10	5	bend
70	5	5	break
	5	10	crack
	10	10	solid
	10	5	crack

In order to study the tribological behaviour—that is, COF and wear—the mechanical properties required for this study are density, hardness, and porosity value. Hence, after a week of curing, the specimen was subjected to the above-mentioned tests.

3.2.1 Density Test

Density is actually the mass per unit volume of a matter. In this study, the density test was done using a Densimeter since it is able to calculate the density of a composite by weighing and submerging the composite into distilled water.

There were no ASTM Standards provided to calculate the density of a composite. Figure 3.4 illustrates the operating flow on how the density test using densimeter.

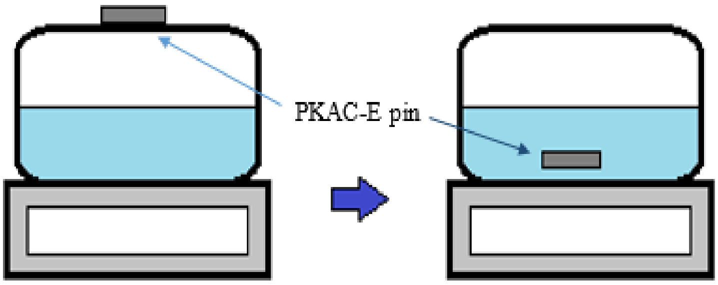

Figure 3.4 Illustration of densimeter usage

First, the Densimeter weighing the composite (dry). Then the Densimeter weighing the submerged composite. By calculating the weight change of the composite with the volume of water changed, the density of the composite was obtained.

This concept were based on Archimedes' principle where it is based on the formula shown in Equation 3.2.

$$\rho = \frac{m}{V} \tag{3.2}$$

Where ρ is the density, m is the composite's mass, and V is the composite's volume.

3.2.2 Hardness Test

Hardness is a measure of how resistant solid matter is to permanent shape change when a compressive force is applied. There are many types of hardness testers, but polymer composites are best tested using Shore hardness durometer. Accordingly, polymer composites such as PKAC-E and others (e.g., truck tyres and safety helmets) are tested using Shore hardness durometer-D type.

While there are actually two types of durometers, which are A-type and D-type, the A-type is more suitable for softer polymer composites, such as door seal and skateboard tyres. Additionally, the hardness value is determined by the penetration of the durometer indenter foot into samples.

Figure 3.5 illustrates how the Shore hardness testing was done. It is based on ASTM D2240: Standard test method for rubber property-Durometer hardness.

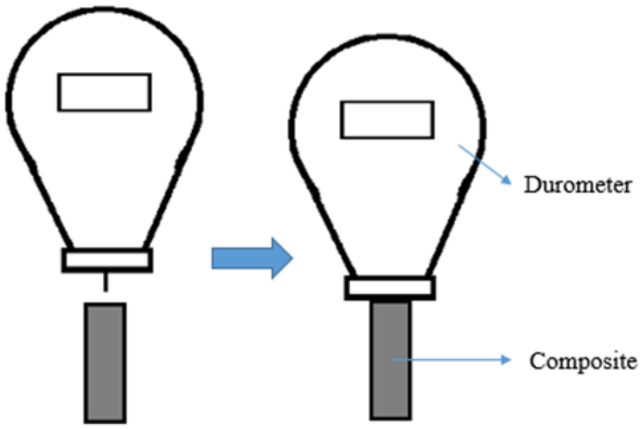

Figure 3.5 Illustration of shore hardness (D-type) testing

3.2.3 Porosity Test

Porosity is the measurement of space or void in a solid matter. In this study, the porosity test was done by submerging the composite into water. First, the composite was weighed, then it was submerged in water until no more air bubbles were escaping from the composite; after which, the composite was re-weighed.

The porosity value was calculated in percentage where the percentage of weight changes was assumed to be filling the hollow part inside the composite. This porosity calculation were also based on Archimedes' principle where the mass of water displaced were calculated.

Hence, the porosity of the composite was calculated following Equation 3.3.

$$porosity\% = \left[\frac{(m_{after} - m_{before})}{m_{after}}\right] \times 100 \qquad (3.3)$$

where m_{after} is the mass of composite after submerged into water, and m_{before} is the mass of composite before submerged into water.

3.3 Tribological Testing

The tribological test done in this study was dry sliding test using pin-on-disc testing by referring to ASTM Standards G99-95a (Appendix B). Because this study required data derived from high temperature, the standard pin-on-disc machine was connected to an external heater. It should be noted, that the heater could only be heated up to 300 ºC.

Furthermore, because of the heat loss to the environment, the highest recorded temperature achieved by the pin was 150 ºC. Moreover, the entire test related to temperature depended on the temperature taken on the external thermometer. The schematic diagram of the pin-on-disc testing and the schematic diagram of the heater to the pin are illustrated in Figure 3.6 and Figure 3.7, respectively.

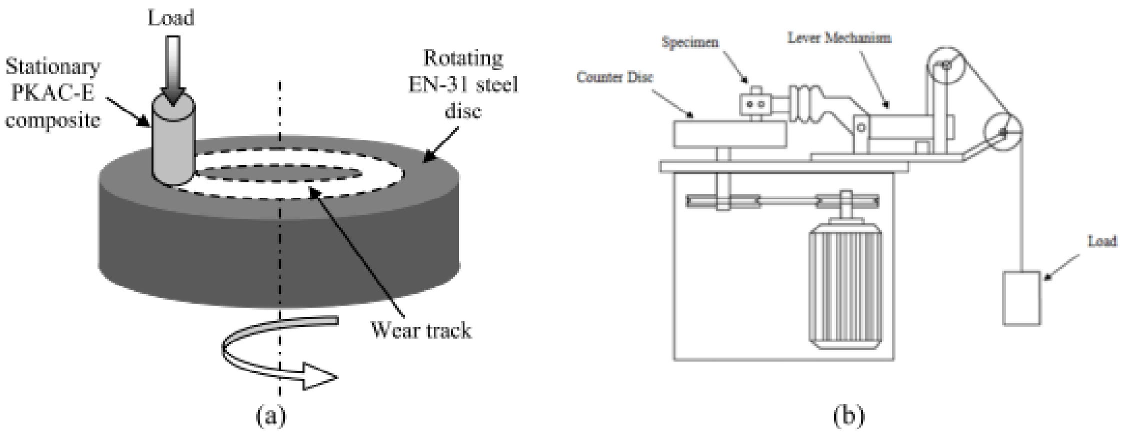

Figure 3.6 (a) Illustration (b) Schematic diagram of pin-on-disc test machine

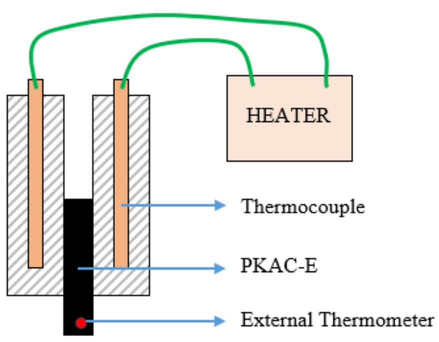

Figure 3.7Schematic diagram of heating flow from heater to pin

Before starting the test, there were some important formulas needed to find the coefficient of friction (COF) and wear rate (k). The equation were called Archard's Equations. The obtained results in the previous section, such as density value, were also used in the formulas. The related formulas are shown in Equation 3.4 to 3.6.

$$COF = \frac{F}{N} \tag{3.4}$$

$$k = \frac{V_{loss}}{WL} \tag{3.5}$$

$$V_{loss} = \frac{m_{before} - m_{after}}{\rho} \tag{3.6}$$

Where *COF* is the Coefficient of Friction, *F* is the applied load, *N* is the normal force, k is the specific wear rate, V_{loss} is the volume loss W is also the applied load, *L* is the sliding distance, *m* is mass, and ρ is the density of pin.

To start the pin-on-disc test, the disc was prepared by first testing the disc with Rockwell hardness tester, following ASTM Standard D785. Then, the disc was polished to the required surface roughness. Likewise, the surface roughness of the disc was tested using a profilometer. After gaining the standard surface roughness required, the disc was submerged into an ultrasonic bath for five minutes. Lastly, the disc was wiped until dry.

The properties of the disc used in this study are shown in Table 3.4.

Table 3.4 Disc Properties

Type	Composition	Hardness	Surface Roughness, Ra
EN-31 steel	C (0.9-1.2%), Si (0.1-0.35%), Mn (0.3-0.75), Cr (1.0-1.6%)	7.9 GPa	0.113 µm

Using sand paper, all pins were grinded according to specified surface roughness and later tested using profilometer. Before installing the pins on to the pin holder, the pins were weighed and after connecting the pin-on-disc to the computer, the test was conducted. The data results from the computer were analysed manually as they were a group of numeric data, and by applying Equation 3.4, the COF was found. Likewise, to calculate the wear rate, the pin was re-weighed once it had finished the sliding test.

Furthermore, by using the mass of the pin before and after the sliding test, Equations 3.5 and 3.6 could be applied into finding the wear rate. It should be noted that all tests were done twice.

Meanwhile, to investigate the tribological behaviour of PKAC-E, the standard method test was done at different sliding distances and temperatures. Other parameters such as compositions, applied loads, sliding speed, and surface roughness were kept constant as shown in Table 3.5.

Table 3.5 Table of tested parameters at tested different distance and temperature

Parameters	value
PKAC Composition (wt %)	70
Applied load (N)	49.05
Surface Roughness, Ra (µm)	0.40 ± 0.02
Sliding Speed (RPM)	500
Sliding Distance (m)	500, 1000, 1500, 2000, 2500
Sliding Temperature (ºC)	27, 90, 150

3.3.1 Determination of Wear and Friction Equations

To determine the equations, larger number of parameters will produce more accurate equations compare to smaller number of parameters. Through the Minitab statistical software, sixteen orthogonal arrays (L_{16}) can be created through five factors (parameters) and four levels (ranges).

Table 3.6 shows the parameters selected and ranges chosen. Those parameters were selected based on previous study and availability of apparatus and technology available. Elaborate explanation were discussed in chapter 4 on how the percentage of the composite were determined.

Table 3.6 Table of parameters and ranges chosen

Composition (PKAC wt. %)	Applied load (N)	Sliding Speed (RPM)	Surface Roughness, Ra (µm)	Temperature on Pin (°C)
60	19.62	1000	0.2	27
65	29.43	1250	0.4	60
70	39.24	1500	0.6	90
75	49.05	1750	0.8	120

From the ranges presented in Table 3.6, the parameters were used to create sixteen orthogonal arrays. The arrays created were presented in Table 3.7. From the sixteen orthogonal arrays created (L16), pin-on-disc test were conducted based on the arrays arrangement.

Table 3.7 L16 Arrays created

No of test	Composition, (PKAC wt%)	Applied Load (N)	Sliding Speed (RPM)	Surface Roughness, Ra (µm)	Temperature on pin (ºC)
1	60	19.62	1000	0.2	27
2	60	29.43	1250	0.4	60
3	60	39.24	1500	0.6	90
4	60	49.05	1750	0.8	120
5	65	19.62	1250	0.6	120
6	65	29.43	1000	0.8	90
7	65	39.24	1750	0.2	60
8	65	49.05	1500	0.4	27
9	70	19.62	1500	0.8	60
10	70	29.43	1750	0.6	27
11	70	39.24	1000	0.4	120
12	70	49.05	1250	0.2	90
13	75	19.62	1750	0.4	90
14	75	29.43	1500	0.2	120
15	75	39.24	1250	0.8	27
16	75	49.05	1000	0.6	60

The test were repeated three times by following the arrays every time the test were conducted. The result collected based on the pin-on-disc test were then analysed based on Equation 3.4 and 3.6. From there, the calculated COF and wear rate for all three trials were analysed using analysis of variance (ANOVA).

Through the ANOVA analysis, the result were presented through means of means and signal to ratios (S/N). Further explanation were discussed at the next sub-section.

The results of the ANOVA analysis were then formed into equations based on regression analysis. Then the equations formed were tested by substituting the orthogonal arrays into the equations.

Comparison between the calculation and experimental were made and from there, the reliability or the equation were calculated by referring to Equation 3.7 and 3.8. The findings for the equation were gained through substitution of the values of parameters and ranges presented at the arrays and compared with the experiment results conducted.

$$error\% = \frac{|Equation - Experiment|}{Equation} \times 100 \qquad (3.7)$$

$$\mathrm{Re}liability\% = 100 - error\% \qquad (3.8)$$

where the error percentage were calculated through the calculation through the difference between the proposed equation values with the experimental values and divided with the equation value. The value were then times with hundred. Meanwhile the reliability percent gained were from controvert of the error value.

3.4 Quantitative Analysis

The quantitative analysis done in this study was more focused on finding the coefficient of friction (COF) and specific wear rate (k) of PKAC-E. The data collected from the pin-on-disc test and the weighing process were calculated and presented through graph plotting. Finally, the collected data results from arrays created were analysed using ANOVA, and from the ANOVA analysis, the statistical equation of friction and wear of PKAC-E were constructed.

3.4.1 Analysis of Variance

ANOVA is statistical analysis that were mainly used for detecting differentials that occurs within the average performance of groups of items tested. ANOVA helps in formally testing the significance of all main factors and their interactions by comparing the mean square against an estimate of the experimental errors at specific confidence levels. The total sum of squared deviations (SST) is calculated as shown in Equation 3.9:

$$SS_T = -\sum_{i=1}^{n} (n_i - n_m)^2 \tag{3.9}$$

where, n_i the number of experiments in the orthogonal array and n_m is the mean S/N ratio for the experiment.

The percentage contribution P can be calculated as according to Equation 3.10:

$$P = \frac{SS_D}{SS_T} \tag{3.10}$$

Where, SSd is the sum of the squared deviations.

A function known as the F test were used to see the most significant effect on design parameters, based on the quality characteristic. Meanwhile, the F-ratio is a ratio of the mean square error to the residual error, and is traditionally used to determine the significance of a factor. The P-value usually reports the significance level, which shows either a suitable or an unsuitable level for the optimization. Contribution (in unit %) is defined as the significance parameter on COF performance.

The ANOVA analysis was done by analysing the collected data on the value of means and signal to noise ratio (S/N). Then, still through ANOVA, the contribution percentage of the tested parameter was obtained. Furthermore, from the percent of contributions parameters, the wear model was extracted using regression analysis.

Regression analysis is a statistical analysis used to estimate relationship among variables, in other words modelling. Regression analysis can be done through either dependent variables or independent variables. Under certain circumstances such as errors when analysing the correlation between parameters or there were no correlations at all.

In the analysis, the data were calculated by referring to the degree of freedom (DOF) of the regression towards other parameters' DOF, and from there, both table of means and S/N ratios can be obtained. From those tables, regression analysis were done. Lastly, the friction and wear equation were constructed.

Pooling method is one solution in solving imbalanced DOF value. The imbalance DOF value occur when the total degree of freedom is higher than the test number. In other words, the test number must be larger than the total degree of freedom. The degree of freedom were calculated by -1 of the level for each parameters [Phadke (1998)].

By having five parameters at four levels, this provides three degree of freedom for each parameters that will results to fifteen degree of freedom. However, to make one analysis close to the reality, degree of freedom for errors also need to be accounted. Hence, by adding another three degree of freedom for errors, the total degree of freedom are exceeding the number of test.

As a solution, pooling method need to be implemented. According to Phadke (1998), "an approximate estimate of error variance can be obtained by pooling the sum of squares corresponding to the factors having the lowest mean square". No replicates are required for the procedure since the sum square due to a factor measures variation between rows of a matrix experiment, not within rows. The next chapter will give a detailed discussion on how pooling method altering the ANOVA analysis.

Due to errors in the DOF that resulting the pooling method solutions, regression analysis are unable to be analysed and only linear analysis can be conducted.

3.5 Qualitative Analysis

The qualitative data from the tests were used in analysing the wear mechanism of the pin with the results obtained in Phase 3. Furthermore, the analysis was done through the aid of SEM and EDX for the wear track analysis and the chemical composition analysis.

In addition, the worn pin was prepared by cutting the residual pin height into 1 mm height, and the cut surface was wiped with sand paper to level the wear surface to the microscope lens. Finally, the pin was placed in the SEM for analysis. It should be mentioned that the best wear track was identified for analysis in EDX. In the EDX analysis, three spectrums were selected from the wear track which were analysed. The best analysis was selected and is presented in the next chapter.

CHAPTER 4

RESULTS AND DISCUSSION

4.1 Mechanical Properties

The average mechanical properties of the composite created are shown in Table 4.1. The mechanical properties obtained were based on several samples tested. The present properties were based on the average value out of three readings. These mechanical properties were considered important because they were used to determine the COF and wear rate. The shown mechanical properties were from 70 wt. % PKAC.

Table 4.1 Mechanical Properties of PKAC-E (70 wt. %)

Hardness (GPa)	Density (g/cm^3)	Porosity (%)
8.8	1.352	1.208

Likewise, the predominant wear mechanism value was based on the mechanical properties value as well. It should be noted that these mechanical properties are only valid at room temperature of 27 °C. This is because the hardness of the PKAC-E varies at higher temperature. Accordingly, the result of the PKAC-E hardness test at different temperatures is shown in Figure 4.1. The error bar presented is based on standard error bars.

In addition, Figure 4.1 shows that the hardness of the composites was reduced almost into half at 150 ºC while it started to decrease rapidly as it approaching 90 ºC. Hence, from these findings, some interesting results were obtained through the tribological test which is discussed in the next sub-chapter.

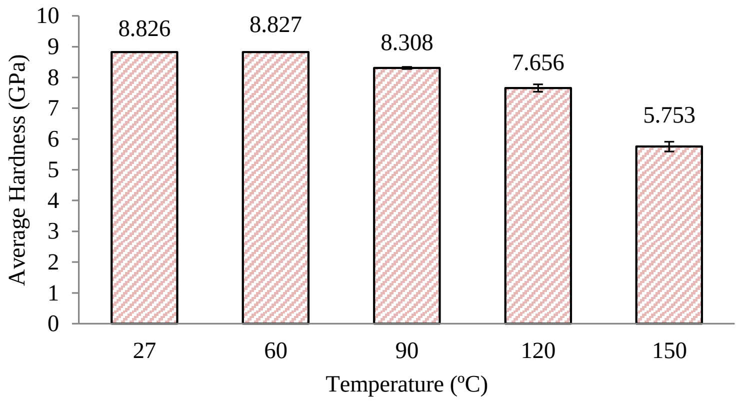

Figure 4.1 Hardness of PKAC-E at different temperatures

Table 4.2 shows that the mechanical properties of the composites differed at different compositions. Accordingly, it was observed that the composite was not usable when the composition of the PKAC was more than 75 wt% and less than 60 wt%. For this reason, the range for composition parameters used were only between 60 wt% and 75 wt%.

Table 4.2 Mechanical properties of PKAC-E at different Composition

PKAC Composition (wt %)	Observation (after fully cured)	Hardness (GPa)	Density (g/cm^3)	Porosity (%)
50	Bend	-	-	-
55	Bend	-	-	-
60	Solid	8.850	1.363	1.275
65	Solid	8.831	1.358	1.231
70	Solid	8.826	1.352	1.228
75	Solid	8.781	1.304	1.640
80	Crack	-	-	-

Moreover, the hardness value, density, and porosity were almost the same between 60 wt%, 65 wt% and 70 wt% of the PKAC; however, it slightly differed for 75 wt%. This could be due to the amount of epoxy used which was not enough to fill in all the gaps and blend through the PKAC particles. For instance, it was observed that as the hardness decreased, the density value also dropped. This is because epoxy density is higher than PKAC density. Accordingly, the change of density value could indicate the change of epoxy value.

Additionally, it was observed through the porosity value where the porosity value suddenly increased. In effect, the increase in porosity value indicated that there was a corresponding increase in the voids or holes inside the composites. This is because, from the virtual observation, the 75 wt% composites takes longer time to fully submerge into the water during the density test compare to the other composition.

So, among 60 wt % to 75 wt%, 70 wt% was selected for different sliding distances and temperatures because the value of hardness, density, and porosity of 70 wt% was almost the same from 65 wt%. Hence, it can be said that the optimum composition for PKAC-E was around 70 wt%.

4.2 Effect on COF and Wear Rate of PKAC-E at Different Sliding Distance

The constant and variable parameters in this study were tabulated as shown in Table 4.3. The Winducom 2008 software was used to record the data from the pin-on-disc test and the data derived was in the form of COF against time function graph.

Table 4.3 Parameter tested for different sliding distance test

Composition	PKAC 70 wt% + E 30 wt%
Applied load	49.05 N
Sliding Speed	500 RPM
Temperature	27 ºC
Surface Roughness	0.4 ± 0.02 µm
Sliding Distance	500-2500 m

Subsequently, the data results were analysed and the average constant COF was taken and presented into a graph of average constant COF against sliding distances. From the graph, it is much easier to understand and see the pattern as well as the average value of the COF. The graph is shown in Figure 4.2. It should be noted that the error bar included is based on standard error bars.

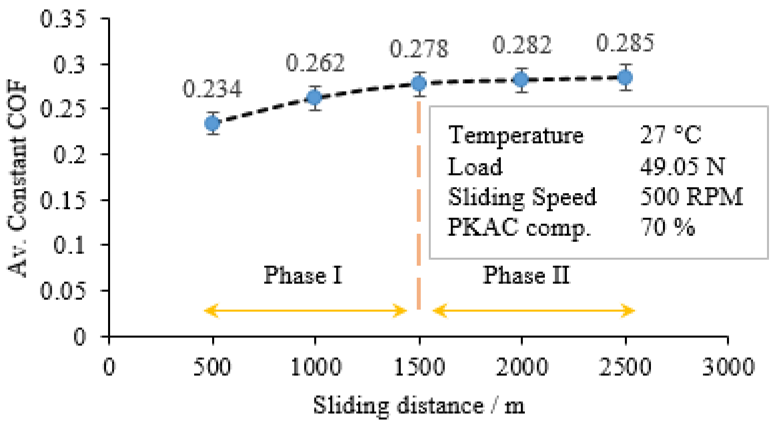

Figure 4.2 Graph of COF against sliding distance

Figure 4.2 shows that the COF value is from 0.234 to 0.285. Furthermore, the graph shows that there was not much difference in the coefficient of friction in all distances. However, when closely analysed, it was found out that the average constant COF only increased at 500m to1500m (Phase I) after which the COF value was almost stable, starting from 1500m to 2500m (Phase II).

At Phase I, the graph shows that there was a small increase in the average constant COF value as the sliding distance increased. Accordingly, it was concluded that the sliding motion could generate heat due to the energy released between the atoms. As the further the distance went, more energy was released due to friction. Hence, the more heat generated. Consequently, the heat generated could cause the composites to break its asperities on contact. Hence, this could be the reason why the COF value increased along with the increase in sliding distance since, generally, heat generated increases with more friction. However, these findings were in contrast with Rao and Das (2011) as they found that COF is not changed by sliding distances.

It was observed, however, at Phase II the COF value started to level off. This finding shows that there are formation of the transfer layer at this sliding condition. In this aspect, it can be said that the findings are in line with Rao and Das (2011). Accordingly, it can be assumed that at Phase I, the process was still at an early stage where the transfer layer was still in the forming process and, at Phase II, the transfer layer had been formed to protect the contacted surface.

Luo (2013) stated that the tribofilm can be generated by various processes which involve mechanical, chemical, and thermal reactions. In this case, the transfer layer was generated from the wear of the soft carbon materials that adhered on the contacted surface and led to a constant or low friction. The experimental proof of the transfer layer formation and details will be discussed through wear mechanism in a later sub-section.

Figure 4.3 shows the specific wear rates against sliding distances. The graph reveals that the specific wear rate decreased as the sliding distance increased. Likewise, the rapid rate of decrease began to slow down as the distance reached 1500m and almost remained constant as sliding distance went farther.

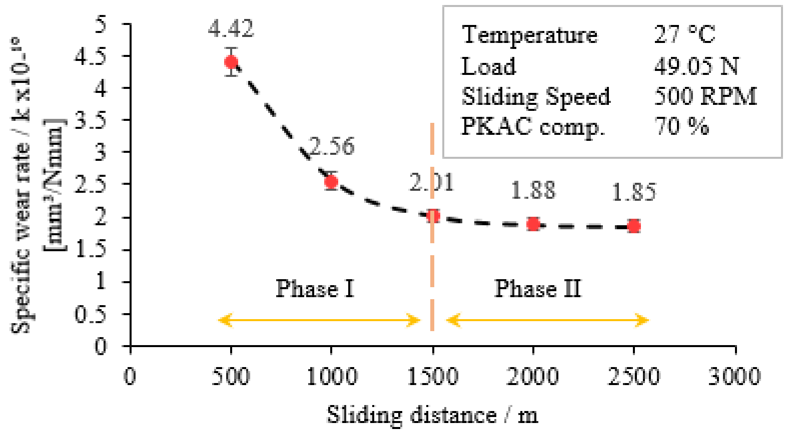

Figure 4.3Graph of specific wear rate against sliding distance

This findings were tallied with the COF result in Figure 4.2. Although the value were decreasing and COF value were increasing, both starts to constant at Phase II. The similarities shows that the transfer layers were formed and turned into the protective layers between the contacting surfaces. Accordingly, the COF and the wear rate value had begun to level off as the transfer layers formed.

4.3 Effect on COF and Wear Rate at Different Temperatures

Table 4.4 shows the tested parameters in this test. From the test, the data derived through the Winducom2008 software on pin-on-disc test was in the form of COF against time function graph. From the graph, the average of the constant COF was taken from each test and tabulated against the tested temperature. The graph of average constant COF against temperature is shown in Figure 4.4. The error bars are shown in standard errors.

Table 4.4 Parameters tested for different temperature test

Composition	PKAC 70 wt% + E 30 wt%
Applied load	49.05 N
Sliding Speed	500 RPM
Temperature	27 - 150 ºC
Surface Roughness	0.4 ± 0.02 µm
Sliding Distance	2500 m

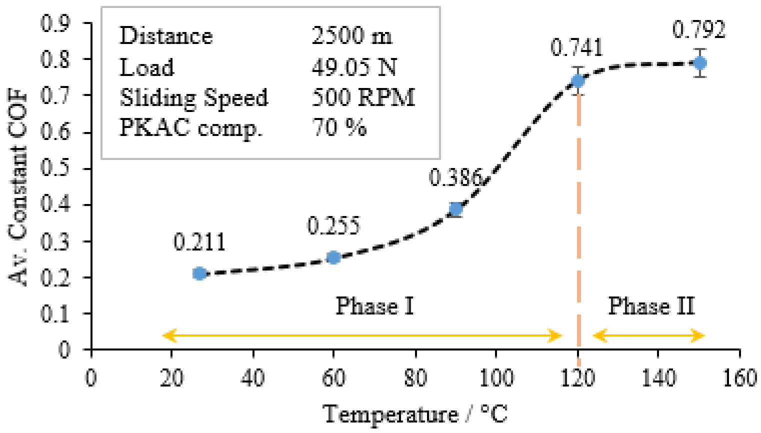

Figure 4.4 Graph of average constant COF against temperature

Figure 4.4 shows that the graph was divided into two phases where Phase I or the thermal degradation phase was from 27°C to120°C and Phase II or the transfer layer formation phase was from 120 °C to 150°C. Phase I shows that the COF increased, but the rate of increase began to taper off as it neared 120 °C. After which, from 120 °C, the COF began to level off and stabilise.

Generally, PKAC-E can act normally without any thermal influence. However, at 60°C, the presence of heat started to weaken the bond of the epoxy element, but not enough to break the PKAC into transfer layer formation. At this rate, the element released was only in the form of debris which was released through the asperities and air due to the tangential force of the rotating disc. In this case, polymer materials produced relatively small amount of debris. According to Brostow et al. (2010), soft materials are known to form little or no debris, especially for polymer based composite.

Additionally, between 90°C to 120°C, the rapid increase in COF indicated that the bond between epoxy and PKAC had weakened. The epoxy component fails and was released as ashes and gas that only seen through observation. Moreover, this was proven as there was an unusual smell and in fact, the gas released was observed during the test. However, the amount of element released was still not enough to form the transfer layer as the COF were not constant. It is significant to note that the rate of increase of the COF began to slow down as the temperature hit 120°C to 150°C.

In this condition, it was concluded that the weakening of the PKAC-E bond had released enough debris to mingle between the asperities of the contacting surface. Hence, the transfer layer might have started to form or might have formed in this condition. Thus, it can be said that at Phase I, the bond of the composite was weakened due to thermal presence and, as a result, the asperities released starting to form the transfer layer at Phase II. The traces of the transfer layer presence can be seen and is discussed in the next sub-chapter.

When referring to Figure 4.5, the wear rate increased at temperature 27°C to 150°C. However, the wear rate started to increase rapidly as the temperature went beyond 120°C. Therefore, it was concluded that as the temperature increased, thermally activated process occurred between the bonds. This thermal activated process resulted in decreasing the hardness of the PKAC-E, and hence increased the specific wear rate value.

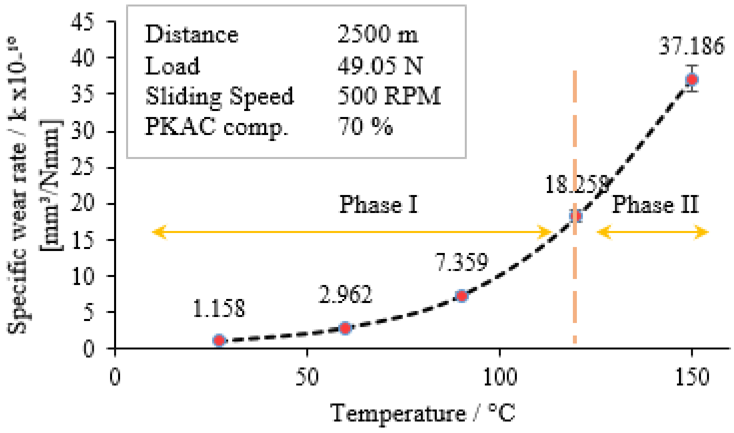

Figure 4.5 Graph of specific wear rate against temperature

For phase I, the increasing in wear rate are lower compared to phase II. This is because as at room temperature towards 120 °C, the composite are maintaining its hardness. However, when it reached around 120 °C, the hardness dropped immediately. This can be said that the composite starts to weaken and began to fails at 120 °C. Although there were small hardness differences within phase I, the wear rate are still increasing. This was believed that the wear are increased not only due to the heat supplied but also from the heat generated through the sliding motion.

The wear rate starts to gradually increase when it is almost at 120 °C towards the end. As stated earlier, the thermal activated process could be seen as the degradation of the epoxy element or binder which is usually pyrolised and oxidised and hence, converted as gas or other degradation products such as debris. This finding is supported through the hardness value data shown in Figure 4.1 of sub-chapter 4.1. As previously shown in Figure 4.1, the hardness value of the composite decreased from 13% and 38% from its original value when heated at 120°C and 150°C, respectively.

Hence, it can be said that hardness is largely responsible for the change of wear rate and COF value. This finding is supported by Brostow et al. (2003) where they found that the temperature had a direct impact on the wear of polymers. This is because, the abrasive wear for polymer is proportional to 1/stress and $(1/(\sigma, \varepsilon))$. However, it is also dependent on the type of polymer.

Gomes et al. (2001) also stated that fatigue effects and frictional heating are likewise responsible for causing surface damage and matrix fracture. According to them, the fibre-matrix bond strength is exceeded and the carbon matrix, which is more brittle than the reinforcement phase and weakly attached to it, is preferentially removed.

4.4 Wear Mechanisms

Through the qualitative approach, the analysis of the worn surface of the pin and the disc was done by using microscopic analysis. The approach used in this analysis was based on SEM, EDX, and surface roughness analysis.

4.4.1 Wear Mechanisms for Different Sliding Distance Test

Figure 4.6 and 4.7 shows the wear track on pin (PKAC-E) composite at 500 m and 2000 m sliding distance. The temperature while conducting this test were at room temperature of 27 °C. The composition of the projected wear track were at 60 wt% of PKAC.

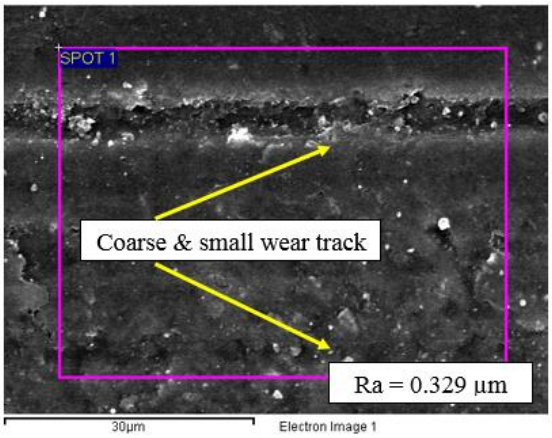

Figure 4.6 Wear track at 500 m sliding distance

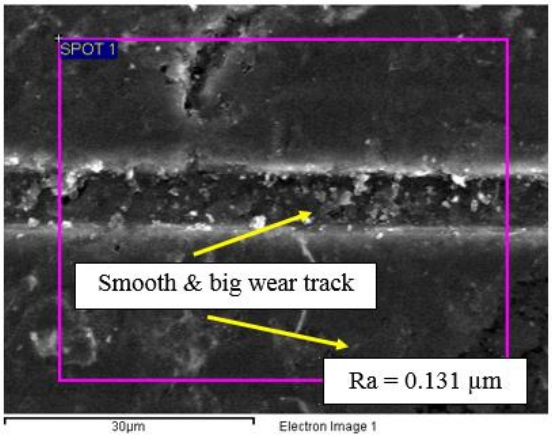

Figure 4.7 Wear track at 2000 m sliding distance

Figures 4.6 and 4.7 both show the worn surface of pin at 27°C which was different at sliding distances of 500 m and 2000 m, respectively. As shown in the microscope image, the wear track formed at Figure 4.6 was coarser and smaller compared to the wear track formed at Figure 4.7 wherein the wear track was smoother and bigger. The coarser wear track (Ra = 0.329 μm) indicated that there was abrasive wear while, on the contrary, the smoother wear track (Ra = 0.131μm) indicated that there was adhesive wear instead.

By comparing both figures, it was concluded that the debris released from abrasive wear filled the asperities at the harder surface and formed the transfer layer as likewise stated by Luo (2013) that tribofilm is defined as a thin solid film generated as a consequence of sliding contact, which is adhered on its parent worn surface but has different chemical composition, structure and tribological behaviour. As a result, data result at 2000m showed smoother track (Figure 4.6) compared to data result at 500 m (Figure 4.7).

The size of the wear track proves that at shorter distance (500 m), the specific wear rate was lower compared to farther distance (2000 m). Moreover, the difference in wear track size supported previous findings in sub-chapter 4.2. Although the specific wear rate increased from the shortest distance to farthest distance, the graph previously shown in Figures 4.2 and 4.3 shows that the transfer layer had just started to form at 1500 m due to the rapid reduction of wear and constant COF. Hence, this result supported the idea that transfer layer had formed at further distance.

4.4.2 Wear Mechanisms for Different Temperature Test

As previously discussed in sub-chapter 4.3, the formation of the transfer layer was due to the breaking of the epoxy bond because of the failure of the composite triggered by the presence of heat or high temperature. This breakage of bond is known as degradation process that usually occurs through pyrolisation.

According to Nguong et.al (2013), pyrolysis is a thermochemical decomposition of materials at elevated temperatures. Pyrolisation occurs when thermally activated process is involved. In general, pyrolysis of organic substances produces gas and liquid products and leaves a solid residue richer in carbon content. As a result, degradation products are released as gas as well as others.

Unfortunately, since it is difficult, if not impossible, to capture or record degradation products, the difference can only be seen through Figures 4.8 and 4.9 which showed the SEM analysis on the wear track at 27 °C and 150 °C, respectively. The wear track image were the wear track of pin (PKAC-E) composite. The composition of the pin analysed below were at 60 wt% of PKAC. The test were conducted at constant sliding distance which at 2500 m. Figure 4.6 and 4.7 shows the wear track on pin (PKAC-E) composite at 500 m and 2000 m sliding distance.

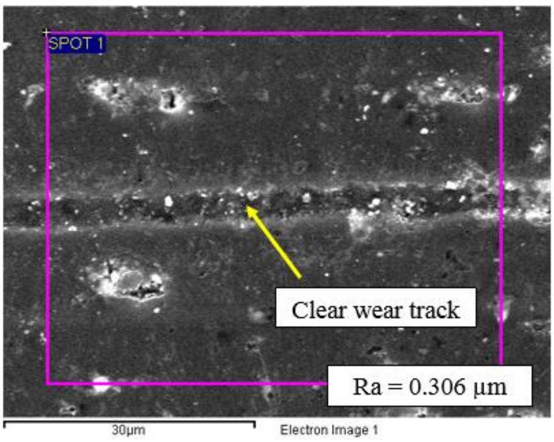

Figure 4.8 Wear track at 27 °C test

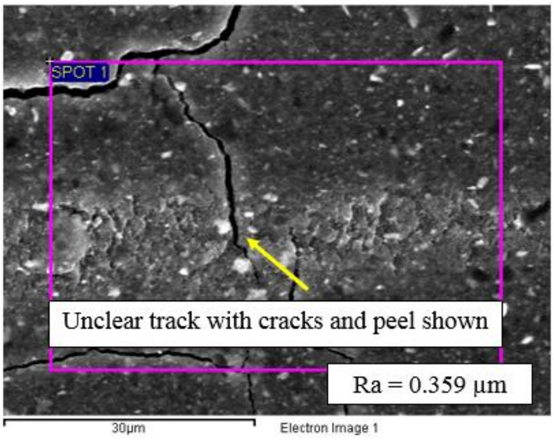

Figure 4.9 Wear track at 150 °C test

From the worn surface in Figures 4.8 and 4.9, it was observed that there were distinct differences between the wear track at 27°C and 150°C. For instance, the wear track for 27°C (Ra = 0.306µm) showed a wear track which indicated the presence of abrasive wear. Meanwhile, at 150°C (Ra = 0.359µm), it was observed that instead of a straight track, the wear track looked as though they were peeling off and cracking. Accordingly, it was concluded that surface fatigue occurred which indicated delamination wear.

Nirmal et al. (2015) stated in his review that delamination wear is predominantly due to polymer swelling. Hence, in this study, although there was no concrete proof that there was delamination wear, the conclusion of the author is based on the theory that delamination is indicated by mild signs of pitting, peel off, and cracks in the worn surface.

Figure 4.10 shows the SEM and EDX analyses of the worn surface of the disc. The disc were analysed with indications of transfer layer formation as there were traces of carbon elements or a black film layer on the disc's surface during the 150°C test. When analysed through SEM, the black element that adhere at the disc shows (bright colour) spot in several areas. By selecting the best image, EDX analysis were done.

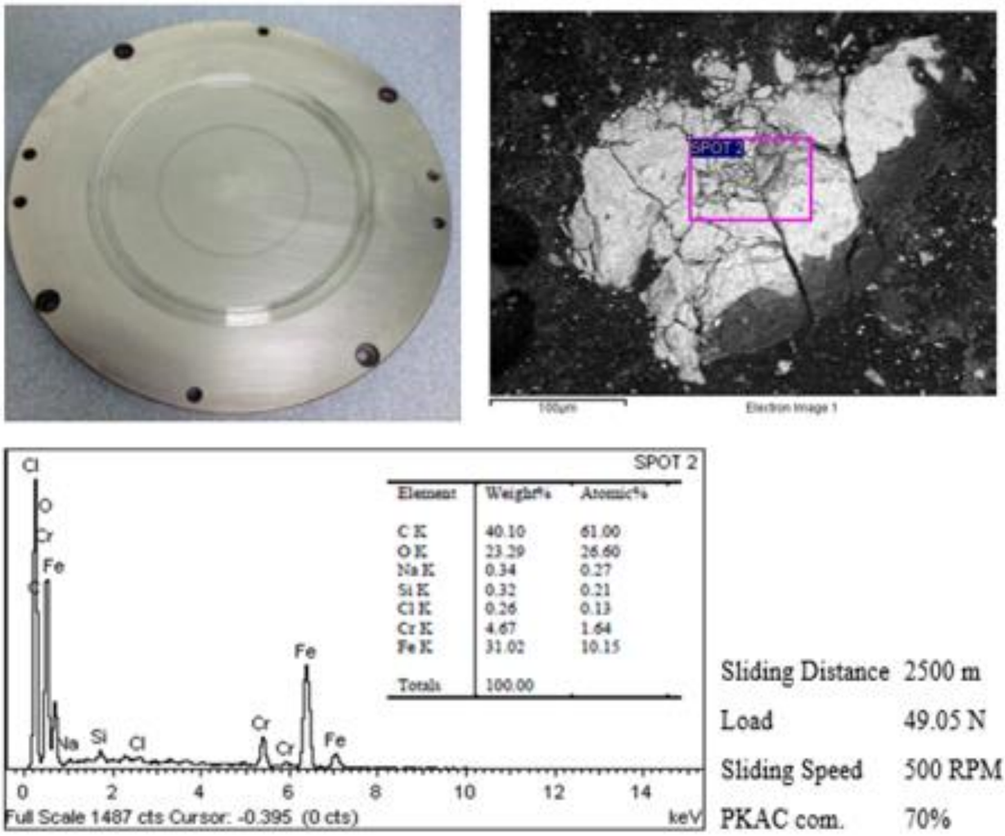

Figure 4.10 SEM and EDX result on disc

Likewise, from EDX analysis, there was 40% carbon element found from the analysed surface. Beside the carbon element, the EDX result also shows some iron, oxygen, and also chromium. The iron element shows were actually the disc element and meanwhile the chromium element were actually the coating element of the SEM itself. Consequently, it can be said that the presence of the transfer layer at 150 °C stabilized the COF.

4.5 Determination of Friction and Wear Equations

In this study, the equations proposed was done through COF analysis and wear rate analysis. For both COF and wear rate analysis, the S/N ratio were selected through "the smaller the better" concept as the main aim of this study was to reduce or eliminate both COF and wear. However, when analysing the data results, some errors occurred which called for reducing the number of factors to be analysed, but nonetheless, without altering any previously collected data.

These errors stemmed from the degree of freedom (DOF) which were calculated based on the theory where the DOF is minus one (-1) from the number of test. The DOF of this study was 15 and in addition, the DOF of each factor/parameter was three. However, when analysed closely, the summation DOF of all five (5) parameters were all equal to 15, which means that the DOF of error was zero.

As a result, the F-value and P-value could not be determined and it should be noted that these values are useful in finding the contribution factors of this study. Accordingly, the table of error display for analysis variance for means and S/N ratios is presented in Table 4.5 and 4.6.

Table 4.5 Errors in Analysis of Variance of means for COF

Source	DOF	Seq SS	Adj SS	Adj MS	F	P	Cont %
Composition (wt%)	3	0.002947	0.002947	0.000982	*	*	63.93
Applied Load (N)	3	0.000107	0.000107	0.000036	*	*	2.32
Sliding Speed (RPM)	3	0.000029	0.000029	0.00001	*	*	0.63
Surface Roughness (µm)	3	0.001473	0.001473	0.000491	*	*	31.95
Temperature (°C)	3	0.000054	0.000054	0.000018	*	*	1.17
Residual Error	0	*	*	*			
Total	15	0.00461					

Table 4.6 Error in Analysis of variance of S/N ratio for COF

Source	DOF	Seq SS	Adj SS	Adj MS	F	P	Cont %
Composition (wt%)	3	7.0874	7.08738	2.36246	*	*	65.16
Applied Load (N)	3	0.1937	0.19371	0.06457	*	*	1.78
Sliding Speed (RPM)	3	0.0575	0.0575	0.01917	*	*	0.53
Surface Roughness (µm)	3	3.3861	3.38612	1.12871	*	*	31.13
Temperature (°C)	3	0.1526	0.15257	0.05086	*	*	1.40
Residual Error	0	*	*	*			
Total	15	10.8773					

Regarding this problem, there is no need to analyse wear considering that the same problem will occur. Rather, the solution was the pooling method. The pooling method suggests that any source of parameter that has a contribution of less than 10% or the least contribution percentage can be eliminated without the need to replicate it. By referring to the contribution value, the least contribution factor was the sliding speed.

Hence, the sliding factor was eliminated and, in so doing, the results showed that the total DOF of the test was 15 with 3 on each factor and 3 for errors.

In addition, a method called F test was used to see the most significant effect on the design parameters based on the quality of the characteristics. Meanwhile, the P-value shows the significance level, whether the level for the optimisation is suitable or not while contribution percentage (cont %) is the percentage of the significance of the factor.

4.5.1 Analysis for Coefficient of Friction

Based on ANOVA analysis done as shown in Tables 4.7 and 4.8, it can be observed that the contribution on mean of mean and mean of S/N ratio was different. Accordingly, S/N ration analysis was selected as there were significant differences in the S/N ratios value.

Table 4.7 ANOVA data for means of COF

Source	DOF	Sum of Squares,SS	Variance	F	P	Cont %
Composition (wt%)	3	0.00295	0.00098	103.12	0.002	63.93
Applied Load (N)	3	0.00011	3.6E-05	3.74	0.154	2.32
Surf. Roughness (μm)	3	0.00147	0.00049	51.56	0.004	31.95
Temperature (°C)	3	5.4E-05	1.8E-05	1.9	0.305	1.17
Residual Error	3	2.9E-05	0.00001			0.63
Total	15	0.00461				

Table 4.8 ANOVA data for S/N ratio of COF

Source	DOF	Sum of Squares,SS	Variance	F	P	Cont %
Composition (wt%)	3	7.0874	2.36246	123.25	0.001	65.16
Applied Load (N)	3	0.1937	0.06457	3.37	0.173	1.78
Surf. Roughness (µm)	3	3.3861	1.12871	58.89	0.004	31.13
Temperature (°C)	3	0.1526	0.05086	2.65	0.222	1.40
Residual Error	3	0.0575	0.01917			0.53
Total	15	10.8773				

The friction equation was determined through the fitted regression analysis. From the table created through regression as shown in Table 4.9, the equation was derived from the coefficient value.

Table 4.9 Regression table for COF

Term	Coef	SE Coef	T-Value	P-Value
Constant	0.0791	0.0476	1.66	0.125
Composition (wt%), C	0.0013	0.00066	1.97	0.075
Applied Load (N), F	-0.000149	0.00034	-0.44	0.666
Surface Roughness (µm), Ra	0.0406	0.0165	2.45	0.032
Temperature (°C), T	0.000012	0.00011	0.11	0.911

As a result, the friction equation can be expressed as:

$$COF = 0.0791 + 0.001300C - 0.000149F + 0.0406Ra + 0.000012T \qquad (4.1)$$

Where C is the PKAC composition (wt%), F is the applied load (N), Ra is the surface roughness (µm), and T is the temperature (°C).

When substituting any number into the equation, we can understand the behaviour of the composite more. Based on the equation, we can see that the coefficient of friction becomes smaller as the load increases. This was supported by Kadiyala (2006) where COF decreased as the load increased. Meanwhile, different situation occurs for surface roughness and temperature. The COF of PKAC-E increased as the surface roughness and temperature increased. According to Lin (2013), the COF increased as the surface roughness increases. This was explained by Findik (2014), at the local asperities, the contact pressure may be determined by the position where eternal deformation happens, although the bulk stress intensity is within the elastic limit.

Hence, it can be said that this equation is only relevant in the plastic deformation region as the COF are not at zero state when there were no load, surface roughness, temperature, and composition applied. The plastic deformation is an early sign of wear. It is was believed that the contact between surfaces of coefficient of friction and wear were at elastic deformation region which the mechanics of contact were obtain based on Hertzian theory.

4.3.2 Analysis for Wear Rate

Based on the ANOVA analysis done as shown in Tables 4.10 and 4.11, it was noted that the contribution on mean of mean and mean of S/N ratio was different. Consequently, S/N ratio analysis was selected as there were significant differences in the S/N ratios' value.

Table 4.10 ANOVA data for mean of wear rate

Source	DOF	Sum of Squares (SS)	Variance	F	P	Cont %
Composition (wt%)	3	104.05	34.68	1.08	0.474	6.05
Applied Load (N)	3	289.06	96.35	3.01	0.195	16.82
Surf. Roughness (µm)	3	89.68	29.89	0.93	0.521	5.22
Temperature (°C)	3	1140.05	380.02	11.88	0.036	66.33
Residual Error	3	95.95	31.98			5.58
Total	15	1718.8				

Table 4.11 ANOVA data for S/N ratio of wear rate

Source	DOF	Sum of Squares (SS)	Variance	F	P	Cont %
Composition (wt%)	3	16.04	5.347	1.12	0.464	2.85
Applied Load (N)	3	47.54	15.848	3.32	0.175	8.44
Surf. Roughness (µm)	3	21.03	7.01	1.47	0.38	3.73
Temperature (°C)	3	464.64	154.88	32.44	0.009	82.44
Residual Error	3	14.32	4.774			2.54
Total	15	563.58				

The wear equation was likewise determined through the fitted regression model. From the table created by the regression shown in Table 4.12, the equation was extracted from the coefficient value.

Table 4.12 Regression table for wear rate

Term	Coef	SE Coef	T-Value	P-Value
Constant	-14.7	22.7	-0.65	0.532
Composition (wt%), C	0.384	0.316	1.22	0.249
Applied Load (N), F	-0.338	0.161	-2.1	0.06
Surface Roughness (µm), Ra	4.23	7.89	0.54	0.602
Temperature (°C), T	0.2126	0.051	4.17	0.002

Hence, the wear equation is:

$$k = -14.7 + 0.384C - 0.388F + 4.23Ra - 0.2126T \qquad (4.2)$$

Where C is the PKAC composition (wt%), F is the applied load (N), Ra is the surface roughness (µm), and T is the temperature (°C).

When substituting any number into the equation, we can understand the behaviour of the composite more. Based on the equation, we can see that the wear rate becomes smaller as the load increases. This was supported by Chua et al. (2013) that wear rate decreased as the applied load increased. However, different situation occurs for surface roughness. The wear rate of PKAC-E increased as the surface roughness decreased. This is due to the breakage of asperities peak that lead to wear.

Hence, it can be said that this equation is only relevant in the plastic deformation region as the wear rate are not at zero state when there were no load, surface roughness, temperature, and composition applied. The plastic deformation are an early sign of wear. It is was believed that the contact between surfaces of coefficient of friction and wear were at elastic deformation region which the mechanics of contact were obtain based on Hertzian theory.

4.5.3 Comparison between Wear and Friction Equation with Experimental Value

From the extracted wear and friction equation, a series of data were calculated by substituting the test parameters from L16 orthogonal arrays into Equations 4.1 and 4.2. Then, the calculated value was directly compared with the experimental value collected previously from the pin-on-disc test by using the same arrays. The experimental and calculated equation data were plotted into graph as shown in Figure 4.11 and 4.12.

Figure 4.11 shows the comparison between the friction equation data with the experimental data for COF, while Figure 4.12 shows the comparison of wear equation data with the experimental data for wear rate. Meanwhile, the reliability of both equations was calculated through Equation 3.7 and 3.8.

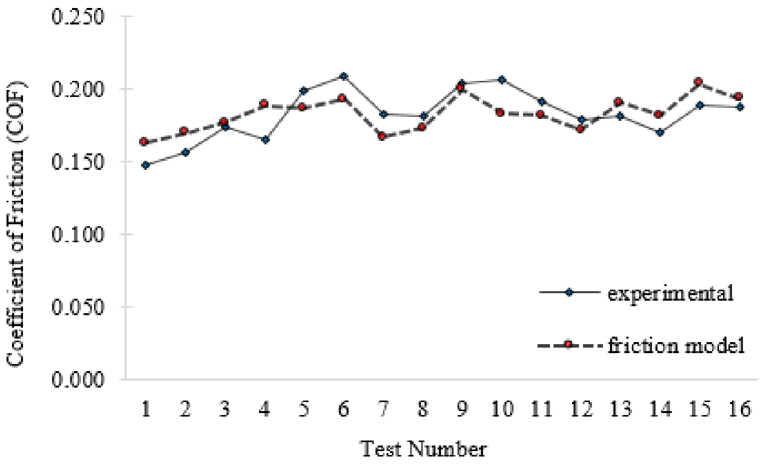

Figure 4.11 Comparison between experimental COF data with friction equation

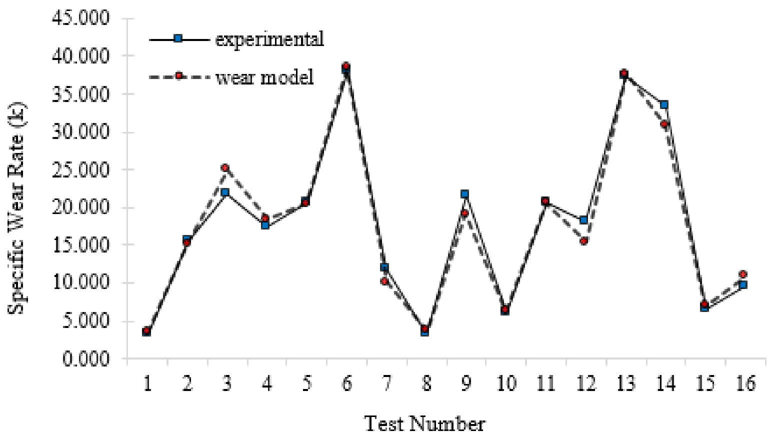

Figure 4.12 Comparison between experimental wear rate data with wear equation

Additionally, by comparing the wear and friction equation with the tabulated experimental data from the pin-on-disc test, it was found that the average error for COF equation were 6.3 % and the average error for wear rate were 9.3 %. The lowest reliability value fall under the wear equation with 90.7 %. The tabulated comparison were presented in Appendix C.

However, the proposed equations was only applicable and limited to the tested and discussed parameters that were within the tested range. It was noted that the equations might vary if the tested parameters and range changed. Meanwhile, the graph pattern are unable to correlate any relation between the COF and the wear rate. The only observation gained were the COF and wear equation shows the same pattern for composition, load, and surface roughness and vice-versa for temperature.

Based on the comparison, the reliability percentage shows how reliable both equations can be used in order to interpolate and predict what happened when the load, composition, temperature, and surface roughness changed. In other words, this models allows researcher to predict the coefficient of friction and wear rate by only substituting the parameters of PKAC-E in the future without any testing needed.

CHAPTER 5

CONCLUSIONS AND RECOMMENDATIONS

5.1 Conclusions

Research on a more efficient lubrication system has been going on for decades. This is best understood in the context of a growing demand for more efficient lubrication system from the machine and automotive industries. Efficient lubricants provide for numerous benefits such as reduction of maintenance cost as well as wear and also accidents that can come from inefficient machine lubricants. More significantly, for the Tribology industry, the availability of natural or indigenous self-lubricating materials is ideal for reducing components of life cycle and reducing environmental pollution as well. However, there is still a substantial knowledge gap in the field of lubricants, but this study gives its share to add to that existing body of knowledge.

Accordingly, this study comes up with the following conclusions:

a) The COF of palm kernel activated carbon epoxy (PKAC-E) is not affected by the sliding distance. Although the COF graph showed a little amount of increment, the value did not change much. In fact, it was between 2.34 to 2.89. Meanwhile, the wear rate was slightly affected by the sliding distance where it was reduced from 4.22×10^{-10} to 1.85×10^{-10} mm^3/Nmm.

   However, the PKAC-E is highly affected by the temperature. Despite the hardness of these materials rapidly reduced at higher temperature, it was there that the potential transfer layer was formed.

b) The predominant wear mechanisms in this study were adhesion of carbon materials onto the disc surface as which caused the formation of transfer film. Also, at higher temperatures, there was the presence of delamination wear due to traces of crack found on the composite's surface.

c) The friction and wear equations proposed in this study shows an average of 9.3 % and 6.3 % of errors respectively between the numerical calculation of both equations from the analysis and the experimental data. The friction and wear equations proposed from this study are:

$$COF = 0.0791 + 0.001300C - 0.000149F + 0.0406Ra + 0.000012T$$

$$k = -14.7 + 0.384C - 0.388F + 4.23Ra - 0.2126T$$

Where C is the PKAC composition (wt%), F is the applied load (N), Ra is the surface roughness (µm), and T is the temperature (°C).

The equations proposed allow researcher to predict the coefficient of friction and wear rate of the PKAC-E composite by only substituting the parameters in the future without any further testing. However, the equations are only valid in plastic deformation region.

5.2 Recommendation for Future Studies

For further studies, several recommendations were suggested by focusing on the following areas:

a) Increase the operating temperature. From the data results, there is the possibility to see the COF and WR value decreasing as the temperature increases.

b) Re-construct the heater and thermocouple position to minimise heat loss to environment. The heater used for the pin was inefficient. For instance, the maximum heat supplied by the heater was 300°C but due to heat loss, the maximum temperature the pin could achieve was around 150°C.

c) Use low density type instead of high density epoxy. High density epoxy, which was used in this study, produced extremely high hardness for the pin. Hence, the hardness of the pin exceeded the hardness of the disc used.

d) Manipulating curing time and PKAC size as alternative to test the surface roughness of pin. Rubbing the pin surface with sand paper (done in this study) consumes a lot of time to obtain the desired surface roughness. Besides, it was believed that this method only affects the wear rate at the beginning of the sliding. At some point, the surface will become smooth. By manipulating the PKAC size and curing process, the grain size and arrangement of elements was different. Through this method, the asperities formed on the surface also differ. Hence leading to different surface roughness.

REFERENCES

Abdollah, M.F.B., Mazlan, M.A.A., Amiruddin, H., and Tamaldin, N., 2013. Frictional Behaviour of Bearing Material under Gas Lubricated Conditions. *Procedia Engineering*, 68, pp.688-693.

Abdollah, M.F.B., Yamaguchi, Y., Akao, T., Inayoshi, N., Miyamoto, N., and Tokoroyama, T., 2012. Deformation-Wear Transition Map of DLC Coating Under Cyclic Impact Loading. *Wear*, 274-275, pp.435-441.

Abdullah, M.I.H.C., Abdollah, M.F.B., Amiruddin, H., Tamaldin, N., Nuri, N.R.M., 2013. Optimization of Tribological performance of hBN/Al2O3 Nanoparticles as Engine Oil Additives. *Procedia Engineering*, 68, pp. 313-319.

Ahmed, N.S., and Nassar, A.M., 2013. Lubrication and Lubricants. Tribology-Fundamentals and Advancements, Intech. Chapter 2, pp.55-76.

Akhlaghi, F., and Zare-Bidaki, A., 2009. Influence of Graphite Content on The Dry Sliding And Oil Impregnated Sliding Wear Behaviour of Al 2024-Graphite Composites Produced By In Situ Powder Metallurgy Method. *Wear* 266(1–2), pp. 37–45.

Alexeyev, N., and Jahanmir, S., 1993. Mechanics of Friction in Self-Lubricating Composite Materials II: Deformation of the Interfacial Film. *Wear*, 166, pp.49-54.

Alexeyev, N., and Jahanmir, S., 1993. Mechanics of Friction in Self-Lubricating Composite Materials I: Mechanics of Second-Phase Deformation and Motion. *Wear,* 166, pp.41-48.

Andersson, B.S., 1991. *Company Perspectives in Vehicle Tribology: Volvo. 17th Leeds-Lyon Symposium on Tribology: Vehicle Tribology*. Tribology Series, Vol. 18, Elsevier Science, Oxford, U.K., pp. 503-506.

Bahadur, S., and Tabor, D., 1985. Role of Fillers in the Friction and Wear Behaviour of High-Density Polyethylene: Polymer Wear and Its Control. *ACS Symposium Series, 287. Washington (DC)*, pp. 253.

Bakry, M., Mousa, M.O.,and Ali, W.Y., 2013. Friction and Wear of Friction Composites Reinforced By Natural Fibers. *Mat.-wiss. u.Werkstofftech*., 44 (1), pp. 21-28.

Biswas, S.K., 2000. Some Mechanisms of Tribofilm Formation in Metal/Metal and Ceramic/Metal Sliding Interactions. *Wear*, 245, pp.178-189.

Blanchet, T.A., and Kennedy, F.E., 1991. Polymer Wear and its Control, American Chemical Society, Washington, DC, *Tribology Trans*. 34 (3), pp.327–334.

Bledzki, A., 1999. Composites Reinforced With Cellulose Based Fibers. *Prog. Polymer Science*, 24(2), pp. 221–74.

Brahmakumar, M., Pavithran, C., and Pillai, R.M., 2005. Coconut Fiber Reinforced Polyethylene Composites: Effect of Natural Waxy Surface Layer of the Fiber on Fiber/ Matrix Interfacial Bonding and Strength of Composites. *Composite Science Technology*, 65, pp. 563–569.

Briscoe, B.J., 1985. Wear of Polytetrafluoroethylene a Maverick or Not: Polymer Wear and its Control. *ACS symposium series 287, Washington (DC)*, pp. 151

Bowman, W., and Stachowiak, G., 1996. Determining the Oxidation Stability of Lubricating Oils Using Sealed Capsule Differentials Scanning Calorimetry (SCPSC). *Tribology International*, 29, pp. 27-34.

Brostow, W., Pietkiewicz, D., and Wisner, S.R., 2007. Polymer Tribology in safety medical devices: Retractable syringes**.** *Advance Polymer Technology*, 26 (56).

Brostow, W., Deborde, J.L., Jaklewicz, M., and Olszynski, P., 2003. Tribology with Emphasis on Polymers: Friction, Scratch Resistance and Wear. *J. Mater*. Ed. 24, 119.

Brostow, W., Kovačevic, V., Vrsaljko, D., and Whitworth, J., 2010. Tribology of Polymers and Polymer-Based Composites. *Journal of Materials Education*, 32 (5-6), pp. 273-290.

Buckley, D.H., 1981. *Surface Effects in Adhesion, Friction, Wear and Lubrication*, Elsevier, Amsterdam, pp. 631.

Donnet,C., and Erdemir, A., 2004. Historical Developments and New Trends in Tribological and Solid Lubricant Coatings. *Surface and Coatings Technology*, 180–181, pp. 76–84.

Dowson, D., 1998. *Hostory of Tribology*, 2nd Edition, Wiley Productions.

Erdemir,V., and Donnet, C., 2001. *Tribology Of Diamond, Diamond-Like Carbon And Related Films*, In Modern Tribology Handbook, Edited by B. Bhushan, CRC Press, Boca Raton. FL, 2, pp. 871-906.

Fernandez-Perez, X., and Igartua, A., 2013. Innovative "Green" Tribological Solutions for Clean Small Engines. *InTech, Open Science*.

Findik, F., 2014. Latest Progress on Tribological Properties of Industrial Materials. *Materials & Design*, 57, pp. 218-244.

Gomes, J.R., Silva, O.M., Silva, C.M., Pardini, L.C., and Silva, R.F., 2001. The Effect of Sliding Speed and Temperature on the Tribological Behaviour of Carbon–Carbon Composites. *Wear*, 249, pp. 240-245.

Goyal, R.K., and Yadav, M., 2013. The Wear and Friction Behaviour of Novel Polytetrafluoroethylene/Expanded Graphite Nanocomposites for Tribology Application. *Journal of Tribology*, 136 (2), pp.1-5.

Grill, A., 1999. Diamond-Like Carbon: State Of The Art, Diamond and Related Materials, 8, pp. 428- 434.

Guy, A., G., 1976. *Essentials of Materials Science*, Mc-Grawhill, New York, USA.

Haq, I., and Bibi, A., 2007. Antiwear Performance of Dicarboxylic Acids in Vegetables Oils. *Tribology Online*, 2, (3), pp. 68-72.

Holmberg, K., Andersson, P., and Erdemir, A., 2012. Global energy Consumption in Passenger Cars. *Tribology International*, 147, pp. 221-234.

Jabatan Penerangan Nasional, 2008. Dasar Automotif Negara. Available at: http://pmr.penerangan.gov.my/index.php/component/content/article/88-dasar-dasar-negara/14195-dasar-automotif-nasional.html [Accessed on January 2014].

Kadiyala, K.C., 2006. Characterization and Tribological Behaviour of Diamond-Like Carbon and Nitrogen-Doped Diamond-Like Carbon Thin Films.

Kapoor, A., Simon, C.T., Shirley, E.S., Priest, M., Rob, S.D., 2001. *Automotive Tribology*, CRC Press LLC.

Kapoor, A. and Franklin, F. J., 2000. Tribological Layers and the Wear of Ductile Materials. Wear, 245, pp. 204-215.

Khedkar, J., Negulescu, I., and Meletis, E.I., 2002. Sliding Wear Behaviour of PTFE composites. *Wear*, 252, pp.361–369.

Kotzalas, M.N., and Doll, G.L., 2010. Tribological Advancements for Reliable Wind Turbine Performance. Philos. *Trans. Royal Soc.Sci*. 368, pp.4829–4850

Lancaster, J.K., 1990. The Lubricated Wear of Polymers. *Wear*, 41(159).

Li, F., Hu, K.A., Lin, J.J., and Zhao, B.Y., 2002. The Friction and Wear Characteristics of Nanometer ZnO Filled Polytetrafluoroethylene. *Wear*, 249(10–11), pp. 877–882.

Lee, L.H., 1985. In: M.J. Comstock (Ed.), *Polymer Wear and its Control*, American Chemical Society, Washington, DC, pp. 27–39.

Lilholt, H., and Lawther, J.M., 2000. *Comprehensive Composite Materials*. Elsevier. pp. 303–325.

Liu, Y., Erdemir, A., and Meletis, E.I., 1996. A Study of the Wear Mechanism of Diamond-Like Carbon Films. *Surface and Coatings Technology*, 82, pp. 48-56.

Ludema, K.C., 1996. Friction, Wear, Lubrication: A Text Book in Tribology. CRC Press, New York.

Luo, Q., 2013. Tribofilms in Solid lubricants. In: Encyclopedia of Tribology. Springer.

Lu, X.C., Wen, S.Z., Tjong, J., Chen, Y.T, and Ren, R.Q., 1996. Wettability, Soil Adhesion, Abrasion and Erosion. *Wear*, 193 (48).

Mizanur, R.M., and Mubarak, A.K., 2007. Surface Treatment of Coir (Cocos Nucifera) Fibers and Its Influence on the Fibers' Physico-Mechanical Properties. *Composites Science and Technology*, 67, pp. 2369–2376.

Myshkin, N.K., Petrokovets M.I, and Kovalev, A.V., 2005. Tribology of Polymers: Adhesion, Friction, Wear, and Mass-transfer. *Tribology International*, 38(910), pp.910-921.

Myshkin, N.K., Petrokovets, M.I., and Kovalev, A.V., 2005. Tribology of Polymers: Adhesion, friction, Wear, And Mass-Transfer. *Tribology International*, 38, 910.

Nakasa,M., 1995, Ebgine Friction Overview. *Proceding International Tribology Conference, Yokohama, Japan*.

Nguong, C.W., Lee, S.N.L., and Sujan, D., 2013. A Review on Natural Fiber Reinforced Polymer Composites. *World Academy of Science, Engineering and Technology*, 73, pp. 1123-1130.

Nirmal, U., Hashim, J., and Mehat Ahmad, M.M.H., 2015. A Review on Tribological Performance of Natural Fiber Polymeric Composites. *Tribology International*, 83, pp. 77–104.

Nosonovsky, M., and Bushan, B., 2010. Surface Self-organisation: From Wear to Self-healing in Biological and Technical Surface. *Applied Surface Science*, 256, pp.3982-3987.

Nosonovsky, M., and Mortazavi, Vahid,. 2012. *Self-Organization at the frictional Interface*. Green Energy and Tribology, Springer.

Pai, R., and Hargreaves, D.J., 2012. *Green Energy and Technology*. Springer-Verlag Berlin Heidelberg, Chapter 13, pp. 347-391.

Paszkowski, M., 2013. *Some Aspects of Grease Flow in Lubrication Systems and Friction Nodes*. Tribology-Fundamentals and Advancements, Chapter 3, pp. 78-106.

Pawlak, Z., 2003. *Tribochemistry of Lubricating Oils*. Elsevier, UK, 45(17).

Pirro, D.M., and Wessol, A.A., 2001. *Lubrication fundamentals*. Marcel Dekker, Inc. New York and Basel 3, 37.

Rae, P.J., and Dattelbaum, D.M., 2004. The Properties of Polytetrafluroethylene in Compression. *Polymer*, 45(22), pp. 7615–7625.

Rao, R., and Das, S., 2011. Effect of Sliding Distance on the Wear and Friction Behaviour of as Cast and Heat-Treated Al–SiCp Composites. *Materials and Design*, 32 (5) pp. 30551-3058.

Rohatgi, P.K., Ray, S., Liu, Y., 1992. Tribological Properties of Metal Matrix-Graphite Particle Composites. *International Materials Rev*., 37(3), pp. 129–152.

Rymuza, Z., 2007. Tribology of Polymers. *Archives of Civil and Mechanical Engineering*. 4 (VII), pp. 177-184.

Sawyer, W.G., Freudenberg, K.D., Bhimaraj, P., and Schadler, L.S., 2003, A Study on the Friction and Wear Behaviour of PTFE Filled with Alumina Nano- particles. *Wear*, 254 (5–6), pp. 573–580.

Sinmazcelik, T., Taskiran, I., 2007, Erosive wear behaviour of polyphenylenesulphide (PPS) composites. *Materials and Design*, 28, pp. 2471-2477

Spikes, H., 2001. Tribology Research in the Twenty-First Century. *Tribology International*, 34, pp. 789-799.

Stachowiak, G.W., and Batchelor, A.W., 2001. *Engineering Tribology*, 2nd Edition, Butter-worth-Heinemann, Boston.

Tabor, D., 1984. Status and Direction of Tribology as a Science in the 80s: Understanding and Prediction, in: *Proceeding International Conference Tribology*, 1, pp. 1–17.

Taylor, C.M., 1998. Automobile Engine Tribology: Design Considerations for Efficiency and Durability. *Wear*, 221(1), pp. 1-8.

Terrel, E.J., Needelman, W.M., and Kyle, J.P., 2012. *Green Tribology and Technology*, Springer. Chapter 13, pp.483-530.

Treutler, C.P.O., 2005. Industrial use of plasma deposited coatings for components of automotive fuel injection systems. *Surf. Coat. Technol*, 200, pp.1969-1975.

Unal, H., Sen, U., and Mimaroglu, A., 2006. An Approach to Friction and Wear Properties of Polytetrafluoroethylene Composite. *Materials and Design*, 27, pp. 694–699.

Voevodin, A.A., Phelps, A.W., Zabinski, J.S., and Donley, M.S., 1996. Friction Induced Phase Transformation of Pulsed Laser Deposited Diamond-Like Carbon, Diamond Related *J. Mater*. 5, pp. 1264–1269.

Vincent, L., and Zambelli, G., 1998. Matériaux et Contacts: Une Approche Tribologique, Presses Polytechniques Universitaires Romandes, Lausanne.

Wei, B., Zhang, B., and Johnson, K.E., 1998. Nitrogen-Induced Modifications in Microstructure and Wear Durability of Ultrathin Amorphous-Carbon Films. *Journal of Applied Physics*, 83 pp. 2491-2499.

Zhou, Z.F., Li, K.Y., Bello, I., Lee, C.S., and Lee, S.T., 2005. Study of Tribological Performance of ECR–CVD Diamond-Like Carbon Coatings on Steel Substrates. *Wear*, 258 (10), pp. 1589-1599.

Zhou, C., Jiao, Y., Chen, Y.K., and Ren, G., 2014. The Tibolligical Properties of Zinz Borate Ultrafine Powder as Lubricant Additive in Sunflower Oil. *Tribology Transections*, 57, pp. 425-434.

BIBLIOGRAPHY

Admile, B., 2014. Application of Taguchi Method for Optimization of Process Parameters for Wear loss of LM25 / Flyash Composite. *International Journal of Innovations in Engineering and Technology (IJIET) Application*, 4(4) pp. 24-39.

Akinci, A., Sen, S., and Sen, U., 2014. Friction and Wear Behaviour of Zirconium Oxide Reinforced PMMA Composites. *Composites Part B: Engineering*, 56. Pp. 42-47.

Baradeswaran, A., and Perumal, A.E., 2014. Wear and Mechanical Characteristics of Al 7075/Graphite Composites. *Composites Part B: Engineering*, 56, pp. 472-476.

Bhatnagar, M.S., 1996. *Epoxy resins (overview) in: The Polymeric Materials Encyclopedia*. CRC Press. pp 1-11.

Bressana, J.D., Darosa, D.P., Sokolowskib, A., Mesquitac, R.A., and Barbosa, C.A., 2008. Influence of Hardness on the Wear Resistance of 17-4 PH Stainless Steel Evaluated By the Pin-On-Disc Testing. *Journal of Materials Processing Technology*, 205, pp. 353–359.

Chowdhury, M. A., Khalil, M. K., Nuruzzaman, D. M., Rahaman, M. L., 2011. The Effect of Sliding Speed and Normal Load on Friction and Wear Property of Aluminum. *Int. Journal of Mechanical & Mechatronics Engineering IJMME-IJENS*, 11, pp.53-57.

El-raghy, T., Blau, P., and Barsoum, M.W., 2000. Effect of Grain Size On friction and Wear Behaviour of Ti3 SiC2. *Wear*, 238, pp. 125-130.

Fernández-pérez, X., Igartua, A., Nevshupa, R., Zabala, P., Zabala, B., Luther, R., Gili, F., and Genovesio, C., 2013. *Innovative Green Tribological Solutions for Clean Small Engines.* Tribology-Fundamentals and Advancements, chapter 10, pp. 275-303.

Funda, K., 2009. The Use of Response Surface Methodology for Prediction and Analysis of Surface Roughness of AISI 4140 Steel. ISSN 1580-2949, pp. 267-270.

Ghaednia, H., and Jackson, R.L., 2013. The Effect of Nanoparticles on the Real Area of Contact, Friction, and Wear. *Journal of Tribology*, 135, Pp. 1-10.

Godfrey, D., 1995. Frictiction Oscillations with a Pin-On-Disc Tribometer. *Tribology International*, 28 (2), pp.119-126.

Kong, L., Zhu, S., Qiao, Z., Yang, J., Bi, Q., and Liu, W., 2014. Effect of Mo and Ag on the Friction and Wear Behaviour of ZrO2 (Y2O3)–Ag–CaF2–Mo Composites from 20°C to 1000°C. *Tribology International*, 78, pp.7-13.

Kuhn, E., 2013. *Friction and Wear of a Grease Lubricated Contact — An Energetic Approach.* Tribology-Fundamentals and Advancements, Chapter 9, pp. 251-271.

Li, W., Zheng, S., Cao, B., and Ma, S., 2011. Friction and Wear Properties of ZrO2/SiO2 Composite Nanoparticles. *Journal of Nanoparticle Research*, 13, pp. 2129-2137.

Maheswaran, P., and Renald, C.J.T., 2014. Investigation on Wear Behaviour of Al6061-Al2o3-Graphite Hybrid Metal Matrix Composites using Artificial Neural Network. *Current Engineering and Technology*, pp. 263-267.

Pintaude, G., 2013. *Introduction of the Ratio of the Hardness to the Reduced Elastic Modulus for Abrasion.* Tribology-Fundamentals and Advancements, chapter 7, pp.217-230.

Sharma, S.C., Girish, B.M., Kamath, R., and Satish, B.M., 1998. Graphite Particles Reinforced ZA-27 Alloy Composite Materials for Journal Bearing Applications. *Wear*, 219, pp. 162-168.

Shibata, K., Yamaguchi, T., Mishima, J., and Hokkirigawa, K., 2008. Friction and Wear Properties of Copper / Carbon / RB Ceramics Composite Materials under Dry Condition. *Tribology Online*, 3 (4), pp. 222-227.

Singh, J., and Chauhan, A., 2014. A Review on Sliding Wear Behaviour of Aluminium Matrix Composites with Hybrid Reinforcements for Automotive Applications. *Tribology Online*, 3, pp. 121-134.

Sivaraos, Milkey, K.R., Samsudin, A.R., Dubey, A.K., and Kidd, P., 2014. Comparison between Taguchi Method and Response Surface. *Jordan Journal of Mechanical and Industrial Engineering*, 8 (1), pp. 35-42.

Society, Japanese. 2014. Diamond-Like Carbon Coating Applied to Automotive Engine Components. *Tribology Online*, 3, pp. 135-142.

So, H., 1996. Characteristics of Wear Results Tested By Pin-On-Disc at Moderatete to High Speeds. *Tribology International*, 29 (5), pp.415-423.

Stanković, M., Vencl, A., and Marinković, A., 2013. A Review of the Tribological Properties of PTFE Composites Filled With Glass, Graphite, Carbon or Bronze Reinforcement. *13th International Conference on Tribology*, pp.135-140.

Stark, W., 2013. Investigation of the Curing Behaviour of Carbon Fiber Epoxy Prepreg by Dynamic Mechanical Analysis DMA. *Polymer Testing*, 32 (2), pp.231-239.

Rodríguez-Tembleque, L., Buroni, F.C., Abascal, R., and Sáez, A., 2013. Analysis of FRP Composites under Frictional Contact Conditions. *International Journal of Solids and Structures*, 50 (24), pp. 3947-3959.

Tauviqirrahman, M., Ismail, R., Jamari, J., and Schipper, D.J., 2013. Artificial Slip Surface: Potential Application in Lubricated MEMS. Tribology-Fundamentals and Advancements, Chapter 8, pp. 231-250.

Taylor, C.M., 1998. Automobile Engine Tribology — Design Considerations for Efficiency and Durability. *Wear*, 221, pp. 1-8.

Uthayakumar, M., Kumaran, S.T., and Aravindan, S., 2013. Dry Sliding Friction and Wear Studies of Fly Ash Reinforced Aa-6351 Metal Matrix Composites. Advances in Tribology, 2013, pp.1-6.

Uvaraja, V.C., Natarajan, N., Rajendran, I., and Sivakumar, K., 2013. Tribological Behaviour of Novel Hybrid Composite Materials Using Taguchi Technique. *Journal of Tribology*, 135, pp.1-12.

Yoon, E.S., Kong, H., Kwon, O.K., and Oh, J.E., 1997. Evaluation of Frictional Characteristics for a Pin-On-Disk Apparatus with Different Dynamic Parameters. *Wear*, 203-204. Pp. 341-349.

Yusoff, Z., and Jamaludin, S.B., 2011. Sliding Wear Properties of Hybrid Aluminium Composite Reinforced by Particles of Palm Shell Activated Carbon and Slag. *Journal of Science and Technology*, pp. 79-96.

Zamri, Y., and Shamsul, J.B., 2011. Physical Properties and Wear Behaviour of Aluminium Matrix Composite Reinforced with Palm Shell Activated carbon (PSAC). *Kovove Mater*, 49, pp. 287-295.

APPENDICES

Appendix A1: Mold used in compression technique to form the composite.

Mold's exploded view with dimensions

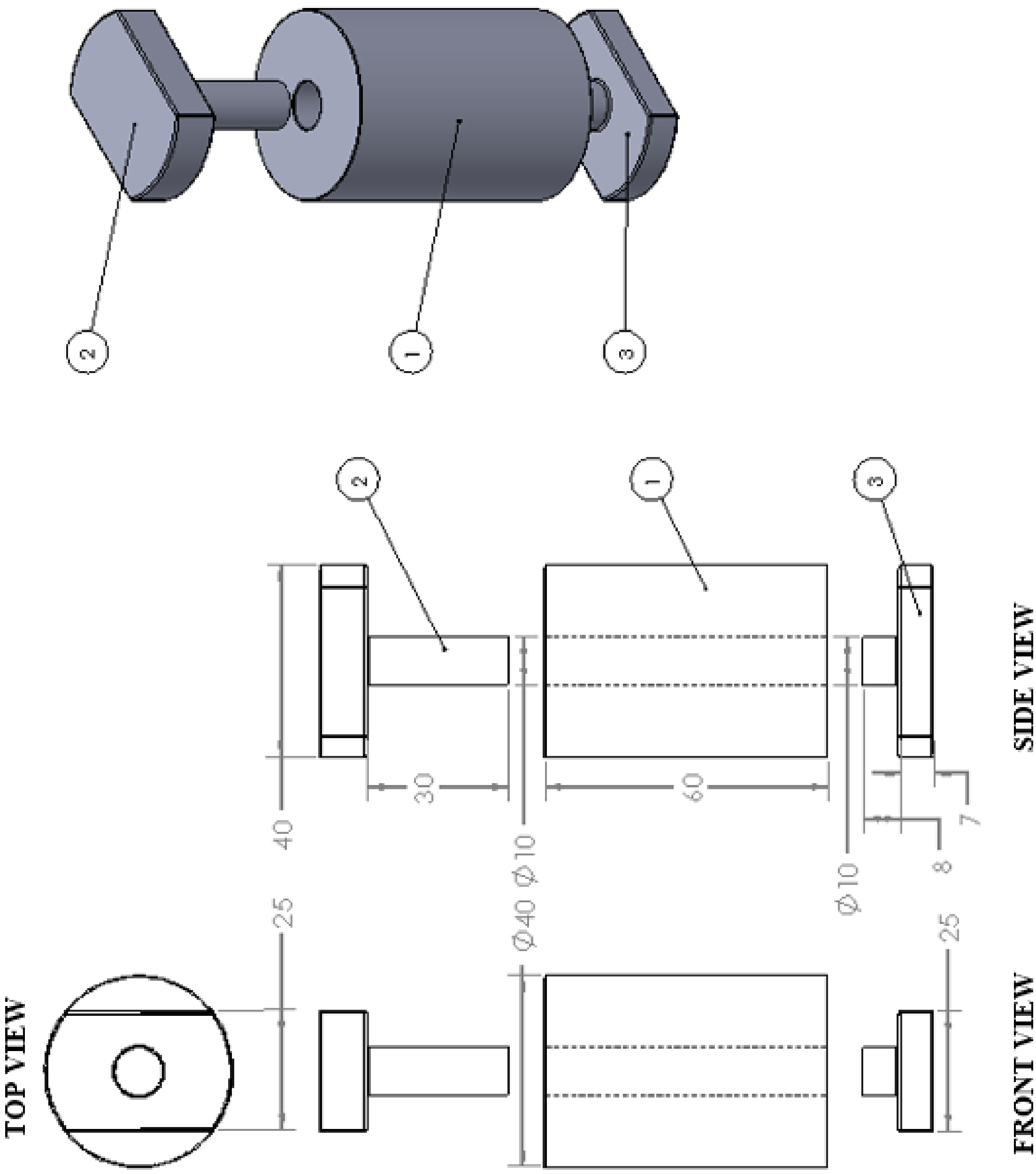

Appendix A2: Mold's exploded view

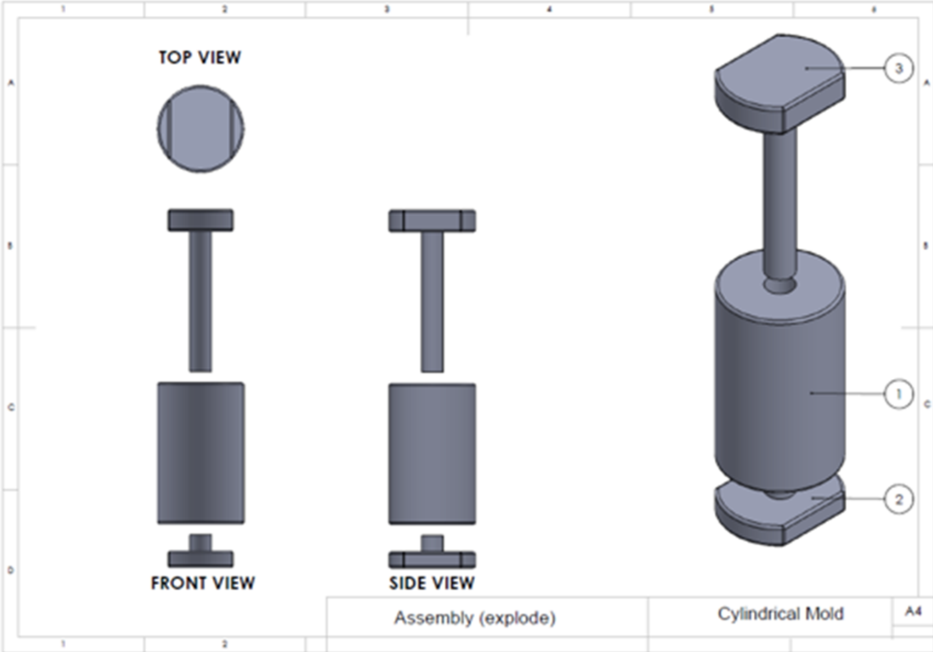

Appendix A3: Bottom part of mold with dimensions

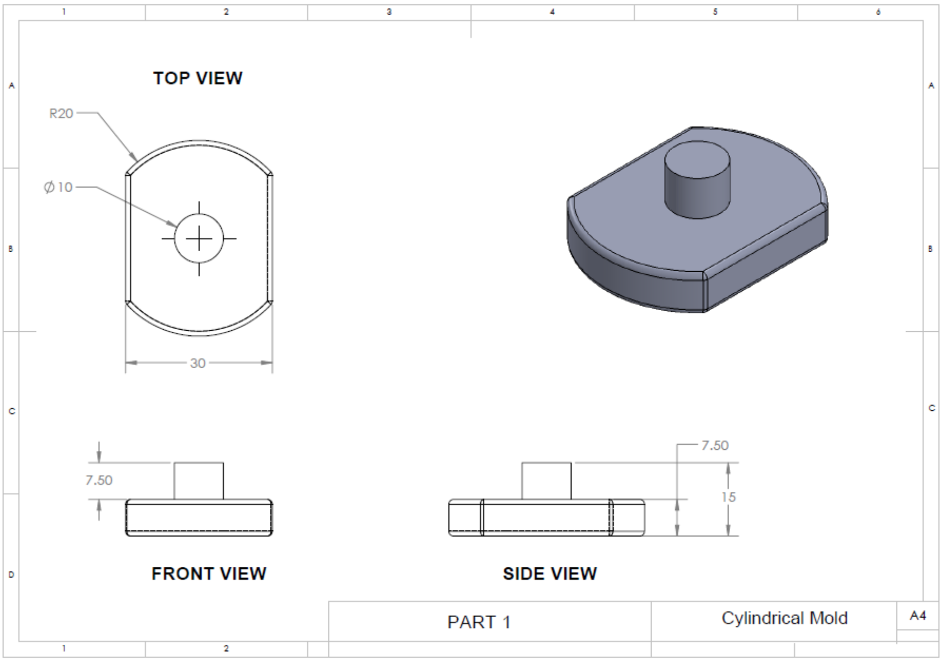

Appendix A4: Body part of mold with dimensions

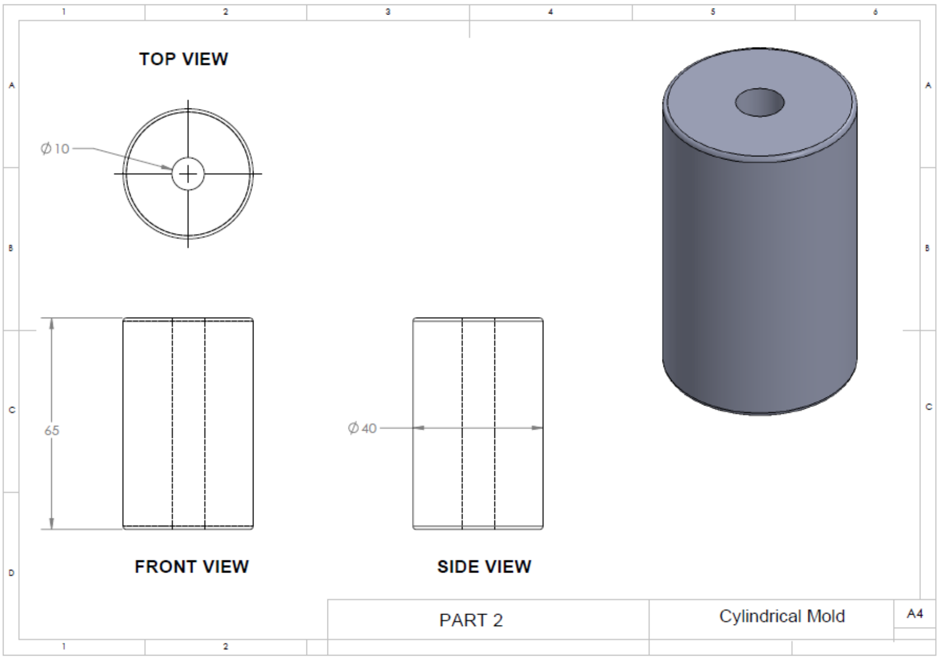

Appendix A5: Upper part of mold with dimensions

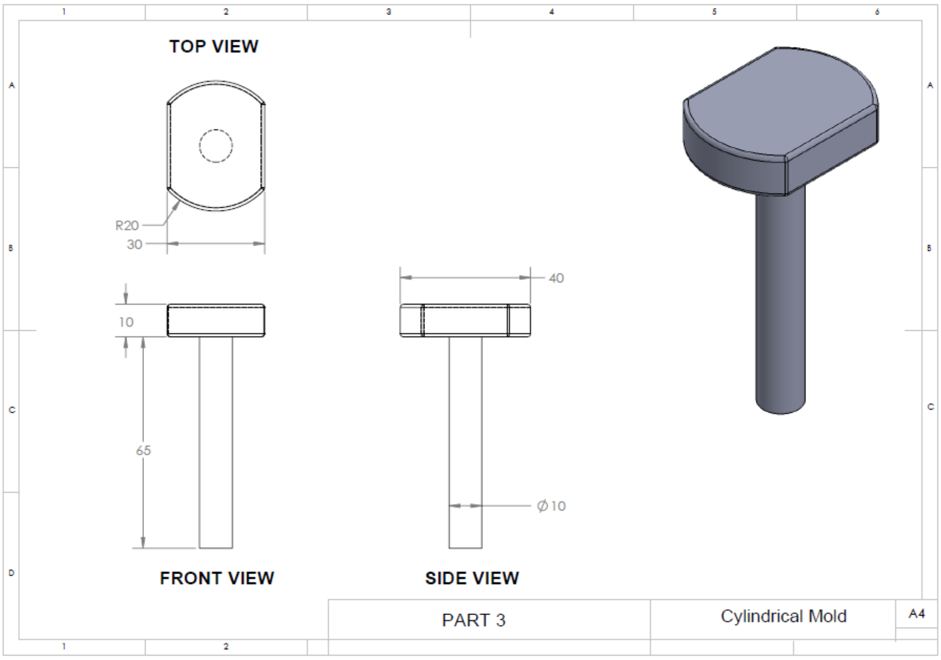

Appendix B1: ASTM standard for pin-on-disc testing (pp. 1)

Designation: G99 – 05 (Reapproved 2010)

Standard Test Method for Wear Testing with a Pin-on-Disk Apparatus[1]

This standard is issued under the fixed designation G99; the number immediately following the designation indicates the year of original adoption or, in the case of revision, the year of last revision. A number in parentheses indicates the year of last reapproval. A superscript epsilon (ε) indicates an editorial change since the last revision or reapproval.

1. Scope

1.1 This test method covers a laboratory procedure for determining the wear of materials during sliding using a pin-on-disk apparatus. Materials are tested in pairs under nominally non-abrasive conditions. The principal areas of experimental attention in using this type of apparatus to measure wear are described. The coefficient of friction may also be determined.

1.2 The values stated in SI units are to be regarded as standard. No other units of measurement are included in this standard.

1.3 *This standard does not purport to address all of the safety concerns, if any, associated with its use. It is the responsibility of the user of this standard to establish appropriate safety and health practices and determine the applicability of regulatory limitations prior to use.*

2. Referenced Documents

2.1 *ASTM Standards:*[2]

E178 Practice for Dealing With Outlying Observations

G40 Terminology Relating to Wear and Erosion

G117 Guide for Calculating and Reporting Measures of Precision Using Data from Interlaboratory Wear or Erosion Tests

2.2 *DIN Standard:*[3]

DIN 50324 Testing of Friction and Wear

3. Summary of Test Method

3.1 For the pin-on-disk wear test, two specimens are required. One, a pin with a radiused tip, is positioned perpendicular to the other, usually a flat circular disk. A ball, rigidly held, is often used as the pin specimen. The test machine causes either the disk specimen or the pin specimen to revolve about the disk center. In either case, the sliding path is a circle on the disk surface. The plane of the disk may be oriented either horizontally or vertically.

NOTE 1—Wear results may differ for different orientations.

3.1.1 The pin specimen is pressed against the disk at a specified load usually by means of an arm or lever and attached weights. Other loading methods have been used, such as hydraulic or pneumatic.

NOTE 2—Wear results may differ for different loading methods.

3.2 Wear results are reported as volume loss in cubic millimetres for the pin and the disk separately. When two different materials are tested, it is recommended that each material be tested in both the pin and disk positions.

3.3 The amount of wear is determined by measuring appropriate linear dimensions of both specimens before and after the test, or by weighing both specimens before and after the test. If linear measures of wear are used, the length change or shape change of the pin, and the depth or shape change of the disk wear track (in millimetres) are determined by any suitable metrological technique, such as electronic distance gaging or stylus profiling. Linear measures of wear are converted to wear volume (in cubic millimetres) by using appropriate geometric relations. Linear measures of wear are used frequently in practice since mass loss is often too small to measure precisely. If loss of mass is measured, the mass loss value is converted to volume loss (in cubic millimetres) using an appropriate value for the specimen density.

3.4 Wear results are usually obtained by conducting a test for a selected sliding distance and for selected values of load and speed. One set of test conditions that was used in an interlaboratory measurement series is given in Table 1 and Table 2 as a guide. Other test conditions may be selected depending on the purpose of the test.

3.5 Wear results may in some cases be reported as plots of wear volume versus sliding distance using different specimens for different distances. Such plots may display non-linear relationships between wear volume and distance over certain portions of the total sliding distance, and linear relationships over other portions. Causes for such differing relationships

[1] This test method is under the jurisdiction of ASTM Committee G02 on Wear and Erosion and is the direct responsibility of Subcommittee G02.40 on Non-Abrasive Wear.

Current edition approved April 1, 2010. Published April 2010. Originally approved in 1990. Last previous edition approved in 2005 as G99–05. DOI: 10.1520/G0099-05R10.

[2] For referenced ASTM standards, visit the ASTM website, www.astm.org, or contact ASTM Customer Service at service@astm.org. For Annual Book of ASTM Standards volume information, refer to the standard's Document Summary page on the ASTM website.

[3] Available from Beuth Verlag GmbH (DIN-- DIN Deutsches Institut fur Normung e.V.), Burggrafenstrasse 6, 10787, Berlin, Germany, http://www.en.din.de.

TABLE 1 Characteristics of the Interlaboratory Wear Test Specimens

NOTE 1—See Note 4 for information.

	Composition (weight%)	Microstructure	Hardness (HV 10)	Roughness[A]	
				R_z (mean) (μm)	R_a (mean) (μm)
Steel ball (100 Cr6) (AISI 52 100)[B] Diameter 10 mm	1.35 to 1.65 Cr ← 0.95 to 1.10 C 0.15 to 0.35 Si 0.25 to 0.45 Mn	martensitic with minor carbides and austenite	838 ± 21	0.100	0.010
Steel disc (100 Cr6) (AISI 52 100)[C] Diameter 40 mm	← <0.030 P <0.030 S	martensitic with minor carbides and austenite	852 ± 14	0.952	0.113
Alumina ball, diameter = 10 mm[D]	← 95 % Al_2O_3 (with additives of TiO_2,	equi-granular alpha alumina with very minor secondary	1610 ± 101 (HV 0.2)	1.369	0.123
Alumina disc, diameter = 40.6 mm[D]	← MgO, and ZnO)	phases	1599 ± 144 (HV 0.2)	0.968	0.041

[A] Measured by stylus profilometry. R_z is maximum peak-to-valley roughness. R_a is arithmetic average roughness.
[B] Standard ball-bearing balls (SKF).
[C] Standard spacers for thrust bearings (INA).
[D] Manufactured by Compagnie Industrielle des Ceramiques Electroniques, France.

TABLE 2 Results of the Interlaboratory Tests[A]

NOTE 1— See Note 4.

NOTE 2—Numbers in parentheses refer to all data received in the tests. In accordance with Practice E178, outlier data values were identified in some cases and discarded, resulting in the numbers without parentheses. The differences are seen to be small.

NOTE 3—Values preceded by ± are one standard deviation.

NOTE 4—Data were provided by 28 laboratories.

NOTE 5—Calculated quantities (for example, wear volume) are given as mean values only.

NOTE 6—Values labeled "NM" were found to be smaller than the reproducible limit of measurement.

NOTE 7—A similar compilation of test data is given in DIN 50324.

Results (ball) (disk)	Specimen Pairs			
	Steel-steel	Alumina-steel	Steel-alumina	Alumina-alumina
Ball wear scar diameter (mm)	2.11 ± 0.27 (2.11 ± 0.27)	NM	2.08 ± 0.35 (2.03 ± 0.41)	0.3± 0.06 (0.3 ± 0.06)
Ball wear volume (10^{-3} mm^3)	198 (198)	...	186 (169)	0.08 (0.08)
Number of values	102 (102)	...	60 (64)	56 (59)
Disk wear scar width (mm)	NM	0.64 ± 0.12 (0.64 ± 0.12)	NM	NM
Disk wear volume (10^{-3} mm^3)	...	480 (480)	...	...
Number of values	...	60 (60)	...	...
Friction coefficient	0.60 ± 0.11	0.76 ± 0.14	0.60 ± 0.12	0.41 ± 0.08
Number of values	109	75	64	76

[A] Test conditions: $F = 10$ N; $v = 0.1$ ms^{-1}, $T = 23°C$; relative humidity range 12 to 78 %; laboratory air; sliding distance 1000 m; wear track (nominal) diameter = 32 mm; materials: steel = AISI 52 100; and alumina = α-Al_2O_3.

include initial "break-in" processes, transitions between regions of different dominant wear mechanisms, and so forth. The extent of such non-linear periods depends on the details of the test system, materials, and test conditions.

3.6 It is not recommended that continuous wear depth data obtained from position-sensing gages be used because of the complicated effects of wear debris and transfer films present in the contact gap, and interferences from thermal expansion or contraction.

4. Significance and Use

4.1 The amount of wear in any system will, in general, depend upon the number of system factors such as the applied load, machine characteristics, sliding speed, sliding distance, the environment, and the material properties. The value of any wear test method lies in predicting the relative ranking of material combinations. Since the pin-on-disk test method does not attempt to duplicate all the conditions that may be

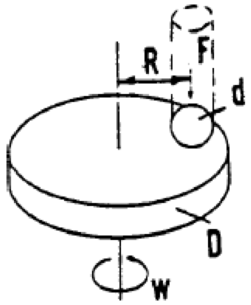

NOTE 1—*F* is the normal force on the pin, *d* is the pin or ball diameter, *D* is the disk diameter, *R* is the wear track radius, and *w* is the rotation velocity of the disk.

FIG. 1 Schematic of Pin-on-Disk Wear Test System

experienced in service (for example; lubrication, load, pressure, contact geometry, removal of wear debris, and presence of corrosive environment), there is no insurance that the test will predict the wear rate of a given material under conditions differing from those in the test.

5. Apparatus

5.1 *General Description*—Fig. 1 shows a schematic drawing of a typical pin-on-disk wear test system.[4] One type of typical system consists of a driven spindle and chuck for holding the revolving disk, a lever-arm device to hold the pin, and attachments to allow the pin specimen to be forced against the revolving disk specimen with a controlled load. Another type of system loads a pin revolving about the disk center against a stationary disk. In any case the wear track on the disk is a circle, involving multiple wear passes on the same track. The system may have a friction force measuring system, for example, a load cell, that allows the coefficient of friction to be determined.

5.2 *Motor Drive*—A variable speed motor, capable of maintaining constant speed (±1 % of rated full load motor speed) under load is required. The motor should be mounted in such a manner that its vibration does not affect the test. Rotating speeds are typically in the range 0.3 to 3 rad/s (60 to 600 r/min).

5.3 *Revolution Counter*—The machine shall be equipped with a revolution counter or its equivalent that will record the number of disk revolutions, and preferably have the ability to shut off the machine after a pre-selected number of revolutions.

5.4 *Pin Specimen Holder and Lever Arm*—In one typical system, the stationary specimen holder is attached to a lever arm that has a pivot. Adding weights, as one option of loading, produces a test force proportional to the mass of the weights applied. Ideally, the pivot of the arm should be located in the plane of the wearing contact to avoid extraneous loading forces due to the sliding friction. The pin holder and arm must be of substantial construction to reduce vibrational motion during the test.

5.5 *Wear Measuring Systems*—Instruments to obtain linear measures of wear should have a sensitivity of 2.5 µm or better. Any balance used to measure the mass loss of the test specimen shall have a sensitivity of 0.1 mg or better; in low wear situations greater sensitivity may be needed.

6. Test Specimens and Sample Preparation

6.1 *Materials*—This test method may be applied to a variety of materials. The only requirement is that specimens having the specified dimensions can be prepared and that they will withstand the stresses imposed during the test without failure or excessive flexure. The materials being tested shall be described by dimensions, surface finish, material type, form, composition, microstructure, processing treatments, and indentation hardness (if appropriate).

6.2 *Test Specimens*—The typical pin specimen is cylindrical or spherical in shape. Typical cylindrical or spherical pin specimen diameters range from 2 to 10 mm. The typical disk specimen diameters range from 30 to 100 mm and have a thickness in the range of 2 to 10 mm. Specimen dimensions used in an interlaboratory test with pin-on-disk systems are given in Table 1.

6.3 *Surface Finish*—A ground surface roughness of 0.8 µm (32 µin.) arithmetic average or less is usually recommended.

NOTE 3—Rough surfaces make wear scar measurement difficult.

6.3.1 Care must be taken in surface preparation to avoid subsurface damage that alters the material significantly. Special surface preparation may be appropriate for some test programs. State the type of surface and surface preparation in the report.

7. Test Parameters

7.1 *Load*—Values of the force in Newtons at the wearing contact.

7.2 *Speed*—The relative sliding speed between the contacting surfaces in metres per second.

7.3 *Distance*—The accumulated sliding distance in meters.

7.4 *Temperature*—The temperature of one or both specimens at locations close to the wearing contact.

7.5 *Atmosphere*—The atmosphere (laboratory air, relative humidity, argon, lubricant, and so forth.) surrounding the wearing contact.

8. Procedure

8.1 Immediately prior to testing, and prior to measuring or weighing, clean and dry the specimens. Take care to remove all dirt and foreign matter from the specimens. Use non-chlorinated, non-film-forming cleaning agents and solvents. Dry materials with open grains to remove all traces of the cleaning fluids that may be entrapped in the material. Steel (ferromagnetic) specimens having residual magnetism should be demagnetized. Report the methods used for cleaning.

[4] A number of other reported designs for pin-on-disk systems are given in "A Catalog of Friction and Wear Devices," American Society of Lubrication Engineers (1973). Three commercially-built pin-on-disk machines were either involved in the interlaboratory testing for this standard or submitted test data that compared adequately to the interlaboratory test data. Further information on these machines can be found in Research Report RR:G02-1008.

8.2 Measure appropriate specimen dimensions to the nearest 2.5 µm or weigh the specimens to the nearest 0.0001 g.

8.3 Insert the disk securely in the holding device so that the disk is fixed perpendicular (±1°) to the axis of the resolution.

8.4 Insert the pin specimen securely in its holder and, if necessary, adjust so that the specimen is perpendicular (±1°) to the disk surface when in contact, in order to maintain the necessary contact conditions.

8.5 Add the proper mass to the system lever or bale to develop the selected force pressing the pin against the disk.

8.6 Start the motor and adjust the speed to the desired value while holding the pin specimen out of contact with the disk. Stop the motor.

8.7 Set the revolution counter (or equivalent) to the desired number of revolutions.

8.8 Begin the test with the specimens in contact under load. The test is stopped when the desired number of revolutions is achieved. Tests should not be interrupted or restarted.

8.9 Remove the specimens and clean off any loose wear debris. Note the existence of features on or near the wear scar such as: protrusions, displaced metal, discoloration, microcracking, or spotting.

8.10 Remeasure the specimen dimensions to the nearest 2.5 µm or reweigh the specimens to the nearest 0.0001 g, as appropriate.

8.11 Repeat the test with additional specimens to obtain sufficient data for statistically significant results.

9. Calculation and Reporting

9.1 The wear measurements should be reported as the volume loss in cubic millimetres for the pin and disk, separately.

9.1.1 Use the following equations for calculating volume losses when the pin has initially a spherical end shape of radius *R* and the disk is initially flat, under the conditions that only one of the two members wears significantly:

$$\text{pin (spherical end) volume loss, mm}^3 = \frac{\pi\,(\text{wear scar diameter, mm})^4}{64\,(\text{sphere radius, mm})} \quad (1)$$

assuming that there is *no significant disk wear*. This is an approximate geometric relation that is correct to 1 % for (wear scar diameter/sphere radius) <0.3, and is correct to 5 % for (wear scar diameter/sphere radius) <0.7. The exact equation is given in Appendix X1.

$$\text{disk volume loss, mm}^3 = \frac{\pi\,(\text{wear track radius, mm})(\text{track width, mm})^3}{6\,(\text{sphere radius, mm})} \quad (2)$$

assuming that there is *no significant pin wear*. This is an approximate geometric relation that is correct to 1 % for (wear track width/sphere radius) <0.3, and is correct to 5 % for (wear track width/sphere radius) <0.8. The exact equation is given in Appendix X1.

9.1.2 Calculation of wear volumes for pin shapes of other geometries use the appropriate geometric relations, recognizing that assumptions regarding wear of each member may be required to justify the assumed final geometry.

9.1.3 Wear scar measurements should be done at least at two representative locations on the pin surfaces and disk surfaces, and the final results averaged.

9.1.4 In situations where both the pin and the disk wear significantly, it will be necessary to measure the wear depth profile on both members. A suitable method uses stylus profiling. Profiling is the only approach to determine the exact final shape of the wear surfaces and thereby to calculate the volume of material lost due to wear. In the case of disk wear, the average wear track profile can be integrated to obtain the track cross-section area, and multiplied by the average track length to obtain disk wear volume. In the case of pin wear, the wear scar profile can be measured in two orthogonal directions, the profile results averaged, and used in a figure-of-revolution calculated for pin wear volume.

9.1.5 While mass loss results may be used internally in laboratories to compare materials of equivalent densities, this test method reports wear as volume loss so that there is no confusion caused by variations in density. Take care to use and report the best available density value for the materials tested when calculating volume loss from measured mass loss.

9.1.6 Use the following equation for conversion of mass loss to volume loss.

$$\text{volume loss, mm}^3 = \frac{\text{mass loss, g}}{\text{density, g/cm}^3} \times 1000. \quad (3)$$

9.2 If the materials being tested exhibit considerable transfer between specimens without loss from the system, volume loss may not adequately reflect the actual amount or severity of wear. In these cases, this test method for reporting wear should not be used.

9.3 Friction coefficient (defined in Terminology G40) should be reported when available. Describe the conditions associated with the friction measurements, for example, initial, steady-state, and so forth.

9.4 Adequate specification of the materials tested is important. As a minimum, the report should specify material type, form, processing treatments, surface finish, and specimen preparation procedures. If appropriate, indentation hardness should be reported.

10. Precision and Bias[5]

10.1 *Statement of Precision:*

10.1.1 The precision of the measurements obtained with this test method will depend upon the test parameters chosen. The reproducibility of repeated tests on the same material will depend upon material homogeneity, machine and material interaction, and careful adherence to the specified procedure by the machine operator. Normal variations in the wear test procedure will tend to reduce the precision of the test method as compared to the precision of such material property tests as hardness or density.

[5] Supporting data have been filed at ASTM International Headquarters and may be obtained by requesting Research Report RR:G02-1008.

10.1.2 Table 2 contains wear data obtained from interlaboratory tests. Mean and standard deviation values are given for all measured quantities.

10.1.3 Statistical analysis (using Guide G117) of the steel vs. steel ball wear scar diameter results for 24 laboratories leads to a mean and standard deviation of 2.14 and 0.29 mm, respectively. The 95 % repeatability limit (within-lab) was 0.37 mm, and the 95 % reproducibility limit (between-labs) was 0.81 mm. Statistical analysis of the steel vs. steel ball friction results for 25 laboratories leads to a mean and standard deviation of 0.60 and 0.11, respectively. The 95 % repeatability limit (within-lab) was 0.19, and the 95 % reproducibility limit (between-labs) was 0.32.

10.2 *Statement of Bias*—No bias can be assigned to these results since there are no absolute accepted values for wear.

10.3 *General Considerations*—Participants in the interlaboratory testing that led to the statements of precision and bias given above involved 28 laboratories, 2 different materials (4 material pairs), 1 test condition, and 3 to 5 replicate measurements each (see Note 4). Subsequent to this testing, data were received from another laboratory that utilized a commercial test machine. These data were found consistent with the results in the interlaboratory study.

NOTE 4—The interlaboratory data given in Table 1 and Table 2 resulted through the cooperation of thirty one institutions in seven countries with the help of national representatives within the Versailles Advanced Materials and Standards (VAMAS) working party on wear test methods.[6]

11. Keywords

11.1 ceramic wear; friction; metal wear; non-abrasive; pin-on-disk; wear

[6] Czichos, H., Becker, S., and Lexow, J., *Wear*, Vol 114, 1987, pp. 109–130 and *Wear*, Vol 118, 1987, pp. 379–380.

APPENDIX

(Nonmandatory Information)

X1. EQUATIONS

X1.1 Exact equations for determining wear volume loss are as follows for:

X1.1.1 A spherical ended pin:

$$\text{pin volume loss} = (\pi h/6)[3d^2/4 + h^2] \tag{X1.1}$$

where:

h = $r - [r^2 - d^2/4]^{1/2}$
d = wear scar diameter, and
r = pin end radius.

Assuming no significant disk wear.

X1.1.2 A disk:

$$\text{disk volume loss} = 2\pi R\,[r^2 \sin^{-1}(d/2r) - (d/4)(4r^2 - d^2)^{1/2}] \tag{X1.2}$$

where:

R = wear track radius, and
d = wear track width.

Assuming no significant pin wear.

Appendix C: Tabulated comparison data between experimental and calculated model

Test no	COF			WR		
	Experimental	Wear model	Error (%)	Experimental, µm ($x10^{-10}$)	Wear model, µm ($x10^{-10}$)	Error (%)
1	0.148	0.163	10.130	03.879	03.295	15.055
2	0.157	0.170	8.280	14.043	12.841	8.559
3	0.174	0.177	1.724	22.429	19.749	11.949
4	0.166	0.184	10.843	16.358	18.657	14.058
5	0.199	0.186	6.532	19.548	21.678	10.899
6	0.209	0.193	7.656	36.811	32.831	10.812
7	0.182	0.167	8.240	12.087	10.599	12.311
8	0.182	0.173	4.945	04.750	04.113	13.418
9	0.204	2.000	1.961	22.647	21.688	4.235
10	0.207	0.190	8.213	06.155	06.511	5.784
11	0.191	0.182	4.712	21.723	21.121	2.771
12	0.179	0.172	3.911	15.632	15.581	0.323
13	0.181	0.191	5.525	35.203	38.295	8.783
14	0.170	0.182	7.059	33.391	30.511	8.625
15	0.189	0.203	7.407	06.456	06.961	7.826
16	0.188	0.194	3.191	09.602	10.815	12.628